

THE PATCH-CLAMP TECHNIQUE EXPLAINED AND EXERCISED WITH THE USE OF SIMPLE ELECTRICAL EQUIVALENT CIRCUITS.*

Dirk L. Ypey¹ & Louis J. DeFelice²

**¹Department of Neurophysiology
Leiden University Medical Center (LUMC)
P.O. Box 9604
2300 RC Leiden, The Netherlands**

voice 31-71-527 6815

fax 31-71-527 6782

email D.L.Ypey@LUMC.NL

**²Department of Pharmacology,
Vanderbilt University Medical Center
Nashville, TN 37232-6600, USA.**

voice 1 (615) 343 6278

fax 1 (615) 343 1679

email lou.defelice@mcm.vanderbilt.edu

* The present chapter is a planned addition to the revised Plenum Press book 'Electrical Properties of Cells' by Louis J. DeFelice. It is a shortened version of a chapter with the same or similar title which may become available on line from Plenum Press under the name PlenumBTOL.

Neither the authors nor Plenum Press take responsibility for either personal damage or damage to equipment that may occur during the practical exercises suggested in this paper.

INDEX

1. INTRODUCTION

- 1.1. What is patch clamping?
- 1.2. Five patch-clamp measurement configurations.
- 1.3. Why use electrical equivalent circuits?

2. FOUR BASIC ELECTRICAL EQUIVALENT CIRCUITS

- 2.1. Charging a capacitor: ERC-circuit I.
- 2.2. Charging a leaky capacitor: ERC-circuit II.
- 2.3. Clamping an ERC-model: ERC-circuit III.
- 2.4. Clamping an ERC cell membrane through a patch pipette: ERC-circuit IV.

3. MODEL CELL EXPERIMENTS

3.1. Introduction

3.2. Model cell and measurement set-up description

- 3.2.1. Equivalent circuit
- 3.2.2. Model hardware
- 3.2.3. Patch-clamp set-up

3.3. Patch-clamp measurement procedures and configurations

- 3.3.1. Switching-on the patch-clamp: amplifier open input capacitance and resistance, and filtering
- 3.3.2. Connecting the pipette holder with pipette to the patch-clamp: extra stray capacity.
- 3.3.3. Immersing the pipette tip to measure pipette capacitance and resistance.
- 3.3.4. Giga-sealing the cell and canceling the fast capacity currents in the cell-attached-patch (CAP) configuration.
- 3.3.5. Making a whole-cell (WC): measuring series resistance and cell capacitance while canceling the slow capacity transients.
- 3.3.6. Pulling an outside-out patch (OOP) and checking the seal resistance.
- 3.3.7. Excision of an inside-out patch (IOP).
- 3.3.8. Making a permeabilized-patch WC (ppWC).

3.4. An instructive model experiment

Checking whole-cell membrane potential and resistance

3.5. Conclusion

REFERENCES

1. INTRODUCTION

1.1. What is patch clamping?

When one hears the words "**patch-clamp**" or "patch-clamping" for the first time in the scientific context, in which this term is so often used (cell physiology and membrane electrophysiology), it sounds like magic or silly jargon. What kind of patch, clamp or activity is one talking about? Obviously, not clamping patches of material together as one might do in patchwork or quilting! "Patch" refers to a small piece of cell membrane and "clamp" has an electro-technical connotation. Patch-clamp means imposing on a membrane patch a defined voltage ("**voltage-clamp**") with the purpose to measure the resulting current for the calculation of the patch conductance. Clamping could also mean forcing a defined current through a membrane patch ("**current-clamp**") with the purpose to measure the voltage across the patch, but this application is rarely used for small patches of membrane. Thus, since the introduction of the patch-clamp technique by Neher and Sakmann in 1976, patch-clamp most often means "voltage-clamp of a membrane patch." Neher and Sakmann applied this technique to record for the first time the tiny (pico-Ampere, pA, $\text{pico} = 10^{-12}$) ion currents through single channels in cell membranes. Others had measured similar single-channel events in reconstituted lipid bilayers. However, the patch-clamp technique opened this capability to a wide variety of cells and consequently changed the course of electrophysiology. That was, at that time, an almost unbelievable achievement, later awarded the Nobel Prize [see the Nobel laureate lectures of Neher (1992) and Sakmann (1992)].

This accomplishment, and the quirky name of the technique, no doubt added to the magical sound of the term patch-clamp. Remarkably, the mechanical aspects of the technique are as simple as gently pushing a 1 μm -diameter glass micropipette tip against a cell. The membrane patch, which closes off the mouth of the pipette, is then voltage-clamped through the pipette from the extracellular side, more or less in isolation from the rest of the cell membrane. For this reason the patch-clamp amplifiers of the first generation were called extracellular patch-clamps.

1.2. Five patch-clamp measurement configurations

Neher and Sakmann and their co-workers soon discovered a simple way to improve the patch-clamp recording technique. They used glass pipettes with super-clean ("fire-polished") tips in filtered solutions and by applied slight under-pressure in the pipette. This procedure caused tight sealing of the membrane against the pipette tip measured in terms of resistance: giga-Ohm sealing, $\text{giga} = 10^9$. This measurement configuration is called **cell-attached patch (CAP)** (see Fig. 1.1), which allowed the recording of single-channel currents from the sealed patch with the intact cell still attached. This giga-seal procedure allowed Neher and Sakmann and their co-workers to obtain three other measurement configurations, including one for intracellular voltage- and current-clamp: the membrane patch between the pipette solution and the cytoplasm is broken by a suction pulse while maintaining the tight seal (Hamill et al., 1981). In this so-called **whole-cell (WC)** configuration (Fig. 1.1), the applied pipette potential extends into the cell to voltage-clamp the plasma membrane. Alternatively, the amplifier could be used to inject current into the cell to current-clamp the cell membrane and to record voltage, for example to study action potentials of small excitable cells, which was impossible until the development of the giga-seal. Another

achievement of the WC-configuration was the possibility to perfuse the intracellular compartment with the defined pipette solution. Although the WC-clamp configuration is no longer a clamp of a small membrane patch, electrophysiologists continued to refer to the WC-clamp configuration as a variant of the patch-clamp technique, probably because the WC-clamp starts with giga-sealing a small membrane patch.

Two other variants are inherent to the patch-clamp technique, since they concern clamping a small area of membrane. The giga-seal cell-attached patch, sometimes called an "on-cell" patch, can be excised from the cell by suddenly pulling the pipette away from the cell. Often the cell survives this hole-punching procedure by resealing of the damaged membrane, so that the excision can be repeated on the same cell. The excised patch is called an **inside-out patch (IOP)** (Fig. 1.1), because the inside of the plasma membrane is now exposed to the external salt solution. This configuration allows one to expose the cytoplasmic side to defined solutions in order, for example, to test for intracellular factors that control membrane channel activity. Another type of excised patch can be obtained, but now from the WC-configuration rather than the cell-attached configuration. It is the **outside-out patch (OOP)**, which is excised from the WC configuration by slowly (not abruptly now!) pulling the pipette away from the WC (Fig. 1.1). This maneuver first defines a thin fiber that eventually breaks to form a vesicle at the tip of the pipette. The configuration obtained is indeed a micro-WC configuration, which allows one to study small populations of channels or single channels and to readily manipulate the "tiny cell" to different bathing solutions for rapid perfusion.

The connection of the current (I) or voltage (V) measuring amplifier to the pipette and the bath is shown in Fig. 1.1 for the OOP, but this connection applies to all other configurations as well. The measuring electrode is inserted in the pipette, while the reference electrode is in the bath. The resulting circuit is shown for the recording of a single OOP channel current, driven by an intrinsic voltage source in the channel and/or a voltage source in the amplifier. The fifth configuration is the **permeabilized-patch WC-configuration (ppWC)** (Fig. 1.1), in which the CAP is not actually ruptured for direct access to the inside of the cell, but made permeable by adding artificial ion channels (monovalent cation channel-forming antibiotics) via the pipette solution (Horn and Marty, 1988). Examples of such antibiotics are amphotericin and nystatin, both produced by microorganisms. The great advantage of this configuration is that it allows intracellular voltage- and current-clamp measurements on relatively intact cells, i.e. cells with a near normal cytoplasmic composition. This is in contrast to the perfused WC-configuration. The various patch-clamp configurations are beautifully described in Neher and Sakmann (1992).

It is the purpose of the present contribution to make the beginning student familiar with the electrophysiological procedures involved in experimenting with each of the five patch-clamp configurations. The required theoretical background will be provided and the explained theory will be exercised with patch-clamp experiments on a model cell designed for teaching and testing purposes.

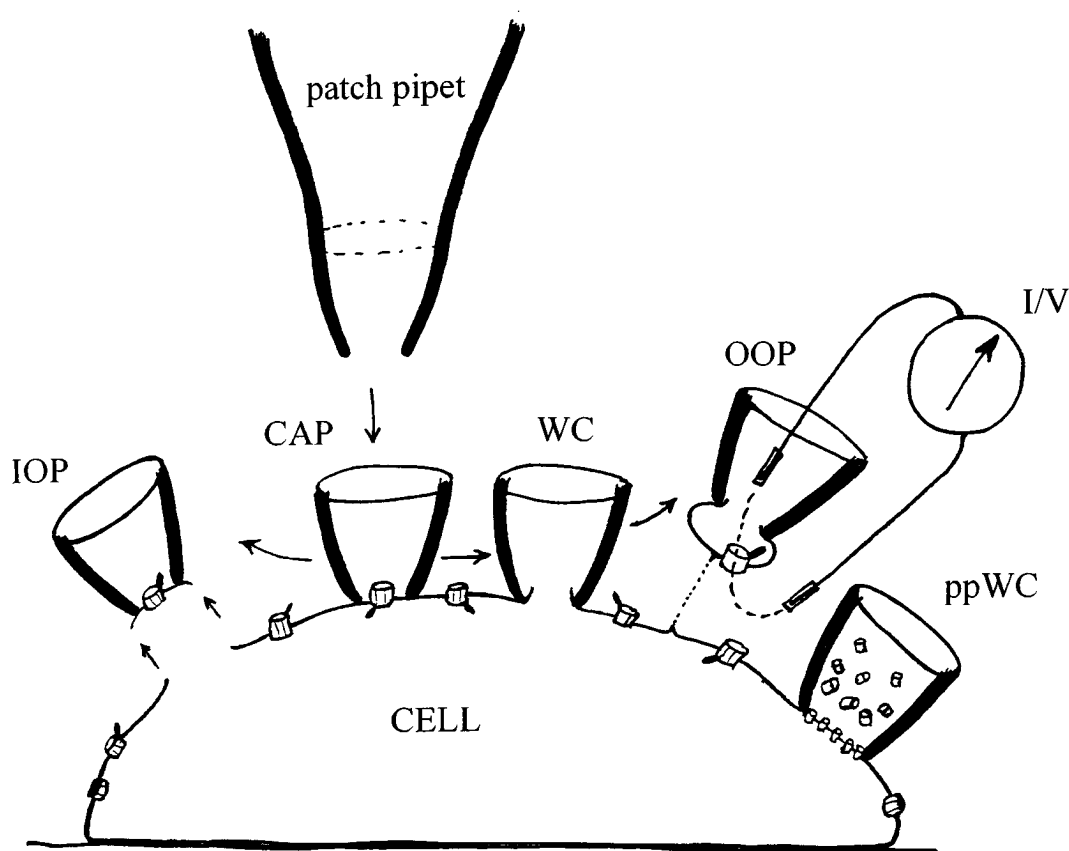


Figure 1.1. Diagram of the five patch-clamp measurement configurations. The figure depicts a living cell seen from the side immersed in extracellular solution and adhered to the substrate. The barrel-type pores in the membrane (some with movable lids or gates) represent ion channels. The five “cups” drawn in semi-perspective close to the cell are the tips of fluid-filled glass micro pipettes connecting the cell to the amplifier. The figure is a composite drawing, as if all five pipettes were placed on one cell. Although this is not a practical possibility, it is possible to make simultaneous two-electrode WC/CAP recordings (see elsewhere in the present book) and CAP/CAP would not be out of the question. All five tips are in position to illustrate how the various measurement configurations are derived from the initial cell-attached-patch (CAP) configuration, established after the giga-sealing procedure. The inside-out patch (IOP) is a CAP excised from the cell membrane. The whole-cell (WC) configuration is obtained by rupturing the CAP. The outside-out patch (OOP) is a vesicle (a “tiny cell”) pulled from the WC configuration. The permeabilized-patch WC (ppWC) develops from the CAP if the pipette solution contains pore-forming molecules incorporating in the CAP. The measuring patch-clamp amplifier and the connecting electrodes, one inside the pipette and one in the bathing solution, are drawn for the OOP-configuration. However, they apply to the other configurations as well. The amplifier measures current (I) through the membrane or voltage (V) across the membrane.

1.3. Why use electrical equivalent circuits?

Patch clamping is an electrical technique, which requires some skill in electrical thinking and measuring. When a patch-clamper is going through the procedures to obtain one of the five measurement configurations, he or she is continuously monitoring voltage-step induced current

responses or current-step induced voltage-responses to check whether the procedures work. While doing that, the experimenter is also continuously conceptualizing the measurement condition as a simple electrical circuit model consisting of resistors (R), capacitors (C), and batteries (E). Because these models are nearly equivalent to the real measurement conditions in certain (but not all!) respects, these models are also called equivalent circuits.

Examples of this way of testing and proceeding are illustrated in Fig. 1.2a. The patch-clamp (pc) amplifier is here represented by a voltage source, E_{pc} , in series with a resistor, R_{pc} , both shunted by an input capacitance, C_{pc} . The measuring patch pipette can be represented by the pipette resistance, R_{pip} , and pipette capacitance, C_{pip} , as soon as the pipette enters the solution. Giga-sealing the patch pipette to the cell membrane can be represented by replacing the direct connection of the pipette with the grounded bath by the seal resistance R_{seal} . After forming the giga-seal, the pipette opening is closed off by the cell-attached patch (CAP) with its high resistance, R_{cap} . Breaking the CAP replaces R_{cap} for access resistance, R_{acc} , providing access to the inside of the whole-cell (WC) with its $E_m:R_m:C_m$ membrane.

Fig. 1.2b shows that the three steps in the procedure for obtaining a WC-configuration can be simulated by a simple ERC-circuit with three switches (S). Closure of S_{pip} (double switch with S_{cpip} and S_{rpip}) would represent entering the bath with the pipette, opening the switch S_{seal} symbolizes (abrupt) sealing, and closure of switch S_{acc} simulates WC-establishment by short circuiting R_{cap} with the access resistance R_{acc} . During actual experiments the experimenter can recognize entering the bath, giga-sealing the cell and making a WC by applying voltage steps in E_{pc} to the pipette and interpreting the current responses as if the circuit of Fig. 1.2b applies. This is the main value of equivalent circuits. The same is true for obtaining the other three patch-clamp configurations discussed above (IOP, OOP, ppWC). Thus, **thinking in terms of simple ERC-circuits is essential** for readily doing the tests and subsequent experiments. Therefore, students interested in learning patch clamping should begin to familiarize themselves with this way of thinking and measuring.

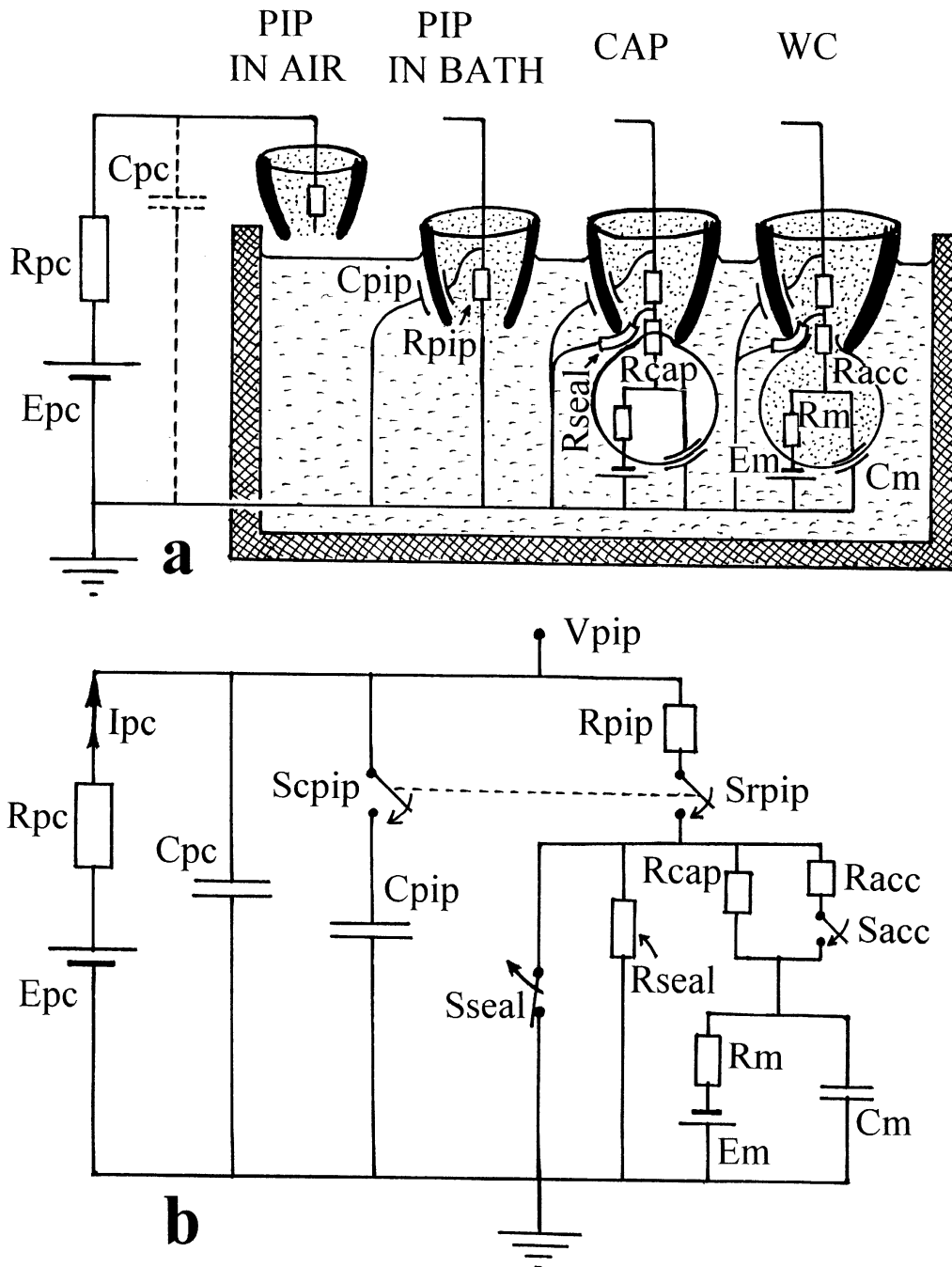


Figure 1.2. A simple electrical circuit modeling the successive patch-clamp procedures for obtaining the whole-cell configuration. A pipette (PIP) entering the bath, forming a giga-seal with the cell, and breaking the cell-attached patch. **Part a** shows how the various components of the circuit can be identified with components of the measurement configuration(s). **Part b** shows the circuit abstracted from the drawing in Part a, including the switches (S) for going through the three successive procedures leading to a WC configuration. The procedures and component names are further explained in the text. During the experiment the quality of the pipette, the giga-seal, and the whole-cell configuration are tested by applying voltage-clamp E_{pc} steps to the pipette and measuring the resulting patch-clamp current I_{pc} .

But how? Studying electronics (Horowitz and Hill, 1990) will help, but this may be an unwanted detour for those students ready to do the experiments. Many electronics courses and textbooks also discuss the properties of inductors, transistors and operational amplifiers, while these subjects are not of major importance for the beginning or even the advanced student in electrophysiology. In our opinion, mastering ERC-circuits should have the highest priority for obtaining measurement skills. The earlier chapters of the present book are particularly devoted to providing the basics of bioelectricity to the beginning student and attempts to fill the gap between basic physical theory and more advanced membrane electrophysiology textbooks (Hille, 2001).

After the present introduction, we begin with the theory of the basic ERC-circuits relevant for patch clamping. Since patch clamping is a technique often used in multi-disciplinary teams of biomedical scientists, students from biology or medicine often want to learn the technique. As they frequently do not have much background in physics or electronic technology, it may be helpful if such students have biological examples of the physics they are learning. Such examples are usually not provided in the general electronics courses. Here we take the opportunity to give such examples while explaining the theory. Fig. 1.2 already shows several important models and the earlier chapters of the present book should help provide the physical basics of ERC components and circuits. We stress, however, that whatever the importance of the theory, practical exercises are as important. Biophysics is an experimental science and trying to recognize ERC-circuit behavior in the electrical behavior of a real circuit or in a living cell is of great instructive value.

Manuals for practical classroom courses on the electronics of ERC-circuits for patch-clamp students are available (Ypey, 1997). However, the most attractive way to become introduced to patch-clamping is to exercise the theory in a real patch-clamp set-up on an equivalent circuit model of a cell showing all the relevant ERC-behavior of a living cell, i.e., with realistic E, R and C values. That is what we do in Chapter 3. It allows the student to combine learning the theory with becoming familiar with a practical set-up. It also forces the student to identify components of a patched cell with electric circuit components (E, R or C). Students ready to start patch clamping may use Chapter 3 as an instruction manual for how to test a set-up in preparation for actual experiments. Reading Chapter 3 before beginning experiments will serve the student more than merely reading the instruction manual of a patch-clamp amplifier, although that should not be forgotten!

To our knowledge, a **structured patch-clamp measurement exercise course** as presented here has not yet become available for general use and teaching. This is in contrast to the many computer programs available for teaching concepts of biophysical or physiological mechanisms. Although these teaching models may be invaluable, in particular for patch-clampers, they do not provide practical measurement exercises. The latter are important because measurement conditions always present practical problems that must be solved before one is able to make sense of the observations.

There are, of course, **limitations** to the model exercises presented here. One is the lack of "wet" (i.e., physical-chemical) properties in the ERC-circuit cell model. Also there is no opportunity to encounter and solve electrode offset or junction potential problems, or to study the ionic dependence of membrane potentials. These topics must be dealt with separately. Another shortcoming of the ERC cell model one should notice is that it lacks Hodgkin-Huxley "excitability" conductance properties. That would be useful, but once able to make reliable measurements, the student will find

that Hodgkin-Huxley teaching models for conceptual training (e.g. Neuron, Ref?, see also PlenumBTOL) are available for further exercises and experiments. A book of great practical use in all aspects of the patch-clamp technique is *The Axon Guide of Sherman-Gold* (1993).

A final comment on limitations: the ERC-circuit with a voltage source E_s in series with an internal source resistor R_s (thus two connection terminals) only applies to patch-clamp stimulation (voltage clamp or current clamp) because the patch-clamp is a true two-terminal input, single-electrode clamp. Although the approach in principle also applies to three-terminal, two-microelectrode voltage-clamp stimulation, this would require some rethinking and redrawing of the measurement configurations. Further justification for using ERC-circuit equivalents in electrophysiology is given in PlenumBTOL.

2. FOUR BASIC ELECTRICAL EQUIVALENT CIRCUITS

In the present chapter we discuss the properties of four simple electrical circuits representing six frequently encountered experimental conditions during patch clamping. For practical and didactic reasons, we discuss these successively as circuits of increasing complexity. Nevertheless, the different situations are rather similar and reduce to two types of basic circuits in many applications, one with one capacitor and the other with two. The simplest circuit, the first one, is most frequently employed during practical experiments. Here it is also used to introduce and explain the equations (Ohm's Law, Kirchoff's Law, and capacitor equation) that describe the behavior of all four circuits. The circuits are denoted as **ERC-circuits**, since they contain batteries (E), resistors (R) and capacitors (C). When introducing the circuits, we will indicate in which respect these circuits can serve as equivalents of practical patch-clamp configurations. The practical use of these circuits will become apparent in demonstrations on the model cell in Chapter 3. Where appropriate, we will discuss important properties of the circuits for real patch-clamp experiments.

Discussion of the four ERC-circuits will serve as preparation for the demonstrations. The theory of the four practical circuits is so important that one can hardly imagine doing patch-clamp experiments without understanding this theory. The circuits will also be used to explain the difference between voltage-clamp and current-clamp stimulation. Although these two stimulation techniques are methodologically very different, technically speaking they are only extremes of one and the same technique. It is very important that the student becomes fluent in switching from voltage-clamp to current-clamp thinking. Some electrophysiologists may rely too heavily on only voltage-clamp, even though voltage-clamp was designed primarily to understand the unclamped behavior of excitable cells. The ERC-circuit approach used here is an excellent way to integrate both ways of clamping in one framework. In a later stage of learning patch-clamp, this approach will help to understand and identify bad voltage-clamp recordings from excitable cells.

2.1. Charging a capacitor: ERC circuit I

Fig. 2.1a gives the most simple battery-resistor-capacitor (ERC) circuit (ERC-circuit I) one can conceive, because it consists of only one battery (E_s), one resistor (R_s) and one capacitor (C), all three components in series in a closed circuit. The index 's' (which stands for 'source') indicates that we consider the $E_s:R_s$ combination as a source that provides the current to charge C. This source may be a voltage- or current-clamp instrument, and C may be the capacity of the patch-clamp input, of a patch pipette or of the membrane of a cell, as illustrated in Fig. 1.2. Before the pipette touches the bath, E_{pc} , R_{pc} , and C_{pc} form the ERC-circuit I. After forming a giga-seal, E_{pc} , R_{pc} , and $C_{pc} + C_{pip}$ again form ERC-circuit I if R_{seal} and R_{cap} are very large. In the whole-cell E_{pc} , $R_{pc} + R_{pip} + R_{acc}$ and C_m may form ERC-circuit I, if R_m and R_{seal} are very large and $C_{pc} + C_{pip}$ very small.

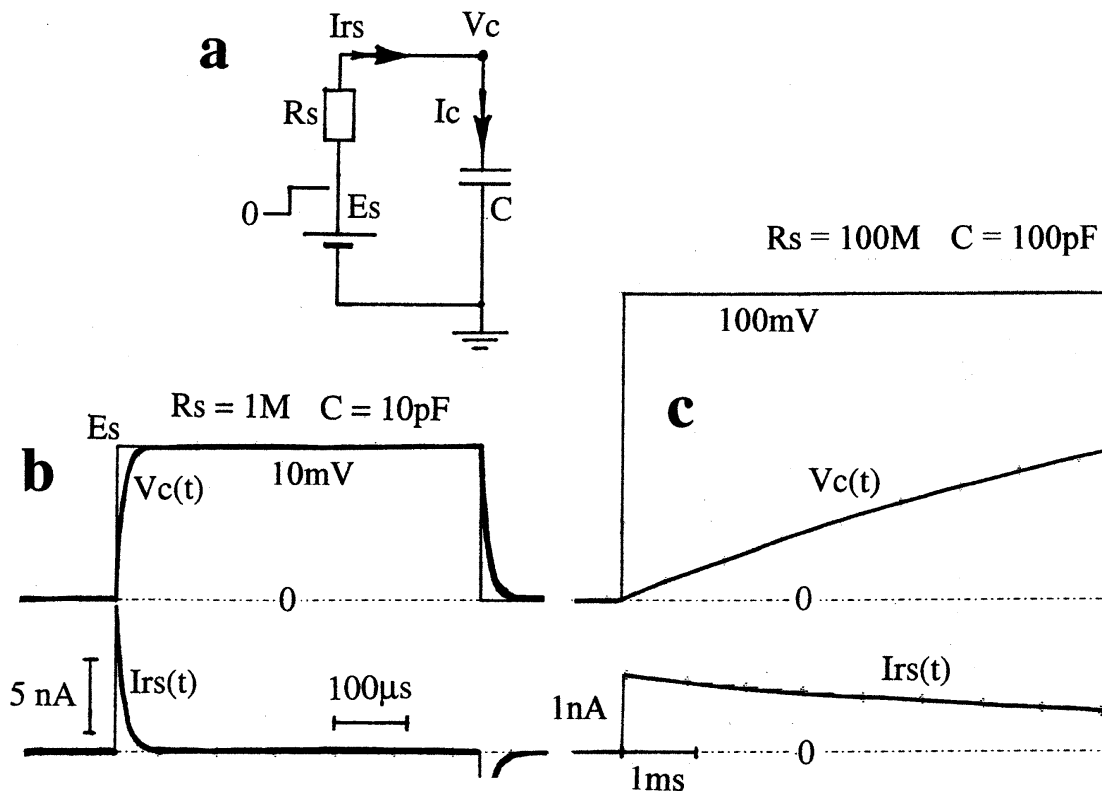


Figure 2.1. Charging a capacitor: ERC-circuit I. Part a shows the ERC-circuit studied, b the voltage-clamp behavior upon an E_s voltage step at a given (low) value of R_s and c the current-clamp behavior of the circuit upon a much higher E_s voltage step at a much higher value of R_s (notice time calibration difference). The upper records of b and c show the E_s voltage steps applied (positive, from zero) and the exponential V_c responses. The lower records show the exponential current responses. Notice that the V_c and I_{rs} transients change with the same time constants and that the current-clamp transients are much slower than the voltage-clamp transients. In both cases there is no stationary current after the transient, since V_c becomes exactly equal to E_s . E_s is the stimulating voltage, I_{rs} is the current through the source resistance R_s , V_c is the voltage across the capacitor C , and I_c is the current flowing into C . The records in panels b and c have been calculated with the use of a computer model of the circuit in a for the component values given in panels b and c.

Here we want to understand how steps in the voltage E_s , as occur during patch-clamp experiments, charge the capacitor: **how rapidly is C charged, by which current, and to what voltage?** We consider step changes in E_s rather than other functions, such as sinusoidal or ramp functions, because step changes are widely used in electrophysiology for membrane stimulation. Electrophysiologists often study how membrane conductance changes when the voltage changes abruptly to a new, fixed value because this is simple to analyze. A quick way to do that is by applying a step change in potential.

We need three equations as mathematical tools to describe the behavior of circuits like Fig. 2.1 (for more theoretical background, see the earlier chapters of the present book). The first formula is **Ohm's law**, $V = RI$, which relates the voltage V (expressed in units of volts, with V as the symbol), across a resistor R (in units of ohms, with Ω as the symbol) to the current I (in units of

amperes, with A as the symbol) flowing through the resistor. You may think of R as proportionality constant between V and I.

It is **convention** in membrane electrophysiology to define intracellular **voltage** and membrane **current polarity** with respect to the ground (= arbitrary 'zero' voltage) on the external side of the membrane. Thus the ground symbols in Figures 2.1-4 indicate the external side of a membrane if the circuit is taken to represent stimulation of a cell with the Es&Rs source. Voltage sources are then positive, if the positive side of the battery is facing the inside of the membrane. Membrane currents are positive when they flow from the inside to the outside, driven by a net positive voltage difference across the membrane.

In our derivations we will often choose positive voltage sources and consider a consistent path of current flow, but the resulting equations will describe voltages and currents for any voltage polarity.

For ERC-circuit I, Ohm's law implies

$$V_{rs} = E_s - V_c = R_s I_{rs} \quad (1a)$$

or

$$I_{rs} = (E_s - V_c) / R_s \quad (1b)$$

with V_{rs} the voltage across R_s , E_s the source battery voltage, V_c the voltage (difference) across the capacitor C and I_{rs} the current through R_s . This equation also applies if V_c and I_{rs} change during charging of C. The way we write 'changing in time' mathematically is $V(t)$, which means that V is changing in time. Then $V_c(t)$ and $I_{rs}(t)$ should be substituted for V_c and I_{rs} , respectively.

The second equation is the **capacitor equation**, $Q = CV$, which relates the voltage V across a capacitor with capacity C (in units of farads, with F as the symbol) to the charge Q (in units of coulombs, with C as the symbol) accumulated on C. Thus C is a proportionality constant in this equation between Q and C. In ERC-circuit I we refer to the voltage across C as V_c to contrast it with V_{rs} . The charge on C we call Q_c . The capacitor equation for circuit I then becomes

$$Q_c = C V_c \quad (2a)$$

or

$$V_c = Q_c / C \quad (2b)$$

This equation means that a given charge Q on a capacitor C causes a greater voltage difference across the capacitor when the capacitor is smaller. On the other hand, a large capacitor holds more charge at a given voltage than a small one.

In ERC-circuit I we want to describe the charging process of C upon a step-change of E_s , thus the changes in Q_c and V_c . We can easily change the capacitor equation from a (static) charge equation to a (dynamic) current equation, because the change in Q_c is exactly equal to the charging current I_c flowing into or out of C. Taken into consideration that a changing charge Q_c (dQ_c/dt) causes a changing voltage V_c (dV_c/dt), Eq. 2 can be rewritten as

$$I_c = dQ_c/dt = C dV_c/dt \quad (3)$$

This equation implies that a constant charging current I_c into capacitor C causes a linearly rising V_c (dV_c/dt constant) across the capacitor. Conversely, when there is a linearly rising V_c , there is a constant charging current.

When E_s in circuit I is stepped from zero V to a constant positive value, while the pre-step $V_c = 0$, a current will start to flow that is determined by Eq. 1, but the same current will change V_c according to Eq. 3. **Kirchoff's law** for currents entering (I_{in}) and leaving (I_{out}) a branching node in a circuit states that $\text{Sum } I_{in} = \text{Sum } I_{out}$. This implies for the simple branching node V_c in circuit I (only one entry and one exit) that:

$$I_{rs} = I_c, \quad (4)$$

and written in full with Eqs. 2 and 3 incorporated:

$$(E_s - V_c)/R_s = C \, dV_c/dt \quad (5a)$$

$$dV_c/dt = -(1/R_s C) (V_c - E_s) \quad (5b)$$

This is a simple, first-order linear **differential equation** relating the change in V_c (dV_c/dt) to V_c , as is more clearly expressed by Eq. 5b. With $V_c > E_s$, dV_c/dt is negative, and it is more negative at smaller R_s and C and at larger $(V_c - E_s)$ values. For $V_c < E_s$, dV_c/dt is positive, and even more positive at smaller R_s and C and at more negative $(V_c - E_s)$ values. At $V_c = E_s$ then $dV_c/dt = 0$, implying steady-state conditions. Therefore V_c moves toward E_s with lower and lower speed the closer it approaches E_s , both from more positive and from more negative values.

Usually, the steady-state value of V_c reached after changing E_s is directly determined from the differential equation by filling in the **steady-state** condition $dV_c/dt = 0$. For that case, Eq. 5 changes to:

$$V_c^* = E_s \quad (6)$$

with V_c^* the steady-state value of V_c . This solution is consistent with the above reasoning based on the properties of the differential equation.

Although the recipe of Eq. 5b is a perfect prescription for the change of V_c during the charging process of C , we would be happier with the **dynamics** of V_c , i.e. the exact **time course** of $V_c(t)$ upon stepping E_s from one voltage to another. This time course $V_c(t)$ is the solution of differential Eq. 5. The actual solution procedure is given in PlenumBTOL. Here, we merely state the end result:

$$V_c(t) = E_s + (V_c(0) - E_s) e^{-t/\tau_s} \quad (7)$$

with

$$\tau_s = R_s C \quad (8)$$

This equation shows that C is charged up from its initial voltage $V_c = V_c(0)$ to the steady-state value $V_c^* = E_s$ (fill in $t = 0$ and $t = \text{very large}$, respectively). The **time constant** $\tau_s = R_s C$ determines how quickly $V_c(t)$ moves toward E_s . The smaller τ_s , i.e. the smaller R_s and C , the faster the V_c transient occurs. Therefore, τ_s is generally used as a characteristic value indicating the charging time of the charging circuit. At $t = \tau_s$, the initial difference between V_c and E_s , $V_c(0) - E_s$, has declined to the value $(V_c(0) - E_s) / e$ (verify this result by filling in $t = \tau_s$). At that exact time, about 60% of the total change of V_c has taken place. After $t = 3\tau_s$, about 95% of the full change has taken place.

Now that we know $V_c(t)$ of the charging process, we can easily determine the **charging current** as a function of time by combining Eqs. 1b and 7:

$$I_{rs}(t) = [E_s - V_c(t)] / R_s = [E_s - V_c(0) e^{-t/\tau_s}] / R_s \quad (9)$$

It is this charging current one sees upon voltage steps during a patch-clamp, voltage-clamp experiment on a very high resistance membrane patch or high resistance whole-cell. The voltage transient $V_c(t)$ is never observed in a regular one-electrode patch-clamp, voltage-clamp experiment, but its time course can be deduced from the current transient. Fig. 2.1b shows the time courses of V_c (Eq. 7) and I_{rs} (Eq. 9) upon a step increase in E_s . The time constants of both transients are the same.

Eq. 9 shows that the charging current is maximal at $t = 0$ and zero at very large t values ($t \gg \tau_s$), consistent with the above differential equation. The peak current at $t = 0$ is $(E_s - V_c(0)) / R_s$, which is equal to E_s / R_s when $V_c(0) = 0$. When only the change in voltage (ΔE_s) and current (ΔI_{rs}) is considered, the ΔI_{rs} peak is equal to $\Delta E_s / R_s$. This is a rule of thumb, which is used during every patch-clamp experiment after breaking the sealed membrane patch to obtain WC-conditions (see demonstration experiments below). This quick calculation serves to decide whether the voltage-clamp conditions of the newly obtained WC are good enough (low R_s) to proceed with the experiment, to try to improve the conditions (lower R_s), or to terminate the experiment and look for another cell. At the same time, one estimates τ_s from the current transient in order to decide whether the rate of current decline, i.e. the rate of charging C of the cell is fast enough to faithfully record subsequent rapidly rising voltage-activated ionic currents. Thus, understanding the properties of simple basic ERC-circuit I is of extreme importance for successfully carrying out any WC patch-clamp experiment!

What does this all mean for obtaining **practical voltage-clamp or current-clamp conditions**? Good clamp conditions are conditions under which the clamped quantity is imposed by the clamping instrument, independent of the properties of the clamped object. Thus, at good voltage-clamp the E_s / R_s instrument clamps C to E_s in circuit I. At good current-clamp the E_s / R_s instrument injects a constant current E_s / R_s into C, with R_s in current-clamp $\gg R_s$ in voltage-clamp. If the purpose of stimulation in ERC-circuit I is to voltage-clamp C to E_s , this stimulus condition results in perfect steady-state voltage-clamp, since V_c becomes exactly equal to E_s (Eq. 6). Whether the voltage-clamp is fast enough to record rapidly activated currents upon the E_s step (which we don't show and do not discuss here), depends on the value of the time constant τ_s . The smaller τ_s , the

better are the dynamic properties of the voltage-clamp, in this case only consisting of the E_s/R_s combination.

The current-clamp conditions in ERC-circuit I are worse. Only at the very beginning just after the step in E_s ($t \ll \tau_s$, with τ_s much larger than in voltage-clamp), is I_{rs} determined by E_s (Fig. 2.1c). Soon after charging C by I_{rs} , the driving force ($E_s - V_c$) declines, suppressing I_{rs} more and more, until I_{rs} has become zero. Thus, while it is impossible with ERC-circuit I to obtain good steady-state current-clamp conditions (at $t \gg \tau_s$), it is impossible to obtain good voltage-clamp conditions just after the step change in E_s ($t \ll \tau_s$).

2.2. Charging a leaky capacitor: ERC-circuit II

Although cell membranes may be very high resistant, they usually have some conductance (the inverse of resistance) in parallel with their capacitance. Thus, mostly we are dealing with capacitance (C) shunted by resistance (R). Such a parallel RC-combination is often called a **leaky capacitor**, as we do here. Fig. 2.2a shows a circuit with a leaky capacitor stimulated by the E_s/R_s source, as in Fig. 2.1a. Thus, the circuit of Fig. 2.2a, ERC-circuit II, is that of Fig. 2.1a with an added R across C .

The RC-part of this circuit looks like a patch pipette, with $R = R_{pip}$ (pipette resistance) and $C = C_{pip}$ (pipette capacitance) (see Fig. 1.2b for switches S_{pip} and S_{seal} closed) or a cell membrane, with $R = R_m$ (membrane resistance) and $C = C_m$ (membrane capacitance), but without a membrane potential (cf. Fig 1.2b for $R_s = R_{pc} + R_{pip} + R_{acc}$, $C_{pc} + C_{pip} = 0$, $R_{seal} \gg R_m$ and $E_m = 0$). The E_s/R_s combination may represent a voltage- or current-clamp used to measure R_{pip} and C_{pip} or R_m and C_m , respectively.

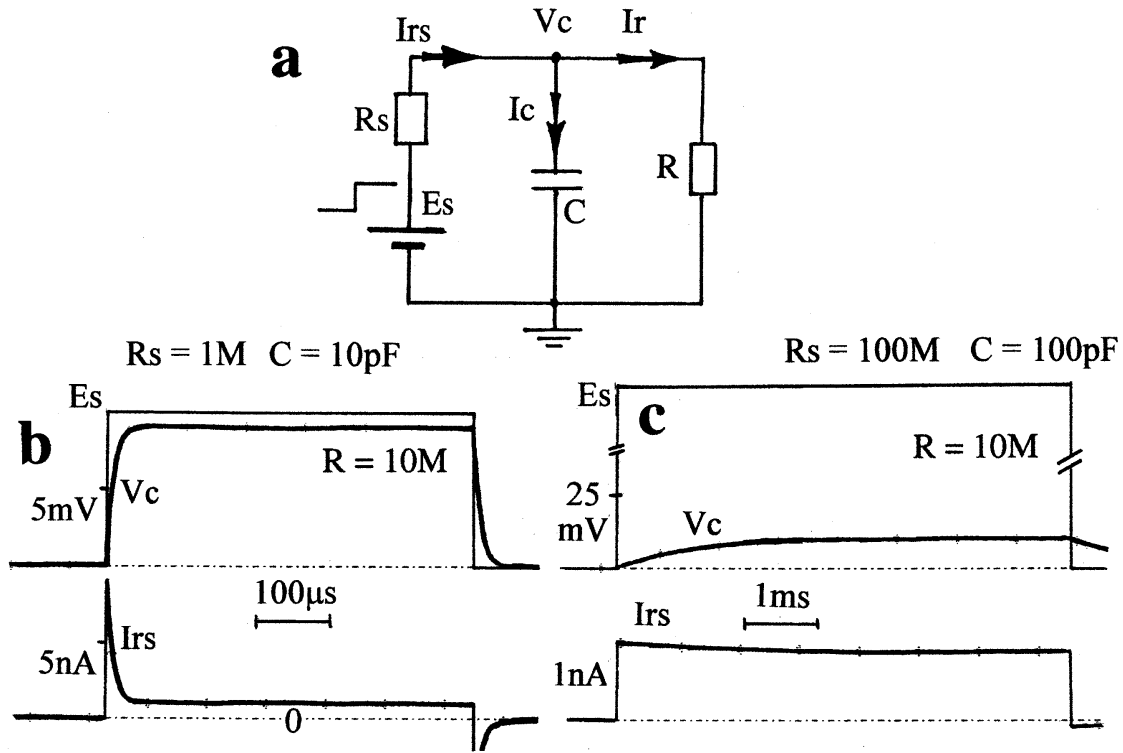


Figure 2.2. **Charging a leaky capacitor: ERC-circuit II.** Circuit (a), record types (b,c) and symbols are as in Figure 2.1 except for an extra component in the circuit, resistance R in parallel to C . It is now the parallel RC-circuit that is voltage-clamped ($R_s \ll R$) (b) or current-clamped ($R_s \gg R$) (c) by the E_s/R_s source. The records have been calculated for the indicated component values. The E_s step in c is 100 mV. The voltage-clamp records at the given resolution do not look very different from those in Fig. 2.1b, but the significant difference is that V_c never becomes exactly equal to E_s and that I_{rs} reaches a stationary value $\sim E_s/R$. It is the value after the capacitance transient that is important during a real patch-clamp experiment, because this value reflects the conductance of the membrane if $R \gg R_s$. This implies that the capacitance peak current is much larger than the current after the peak transient. The current-clamp records look very different from those in Fig.2.1c. I_{rs} reaches a stationary value $E_s/(R_s + R) \sim E_s/R_s$ and V_c shows a stationary displacement $\sim I_{rs}R$. The time constant is now smaller than for ERC-circuit I: $\sim RC$ in stead of R_sC .

We investigate the behavior of the ERC-circuit II in the same way as we did for ERC-circuit I: **we want to know $V_c(t)$ and $I_{rs}(t)$ upon a step in E_s .** The equations for I_{rs} and I_c are the same as for circuit I, but we have now one current more, the current I_r through the added R , which is, according to Ohm's law, equal to

$$I_r = V_c / R \quad (10)$$

Branching node V_c has one entry current (I_{rs}) but two exit currents (I_c and I_r). So, application of **Kirchoff's current law** results in

$$I_{rs} = I_c + I_r \quad (11)$$

By substitution of the equations for the three currents (Eqs. 1b, 3 and 10), one obtains again the **differential equation** describing the change in V_c (dV_c/dt) upon E_s steps

$$(E_s - V_c) / R_s = C \, dV_c / dt + V_c / R \quad (12a)$$

or

$$dV_c / dt = (-1 / \tau_{sp}) \cdot (V_c - V_c^*) \quad (12b)$$

with

$$V_c^* = R \, E_s / (R_s + R) \quad (13)$$

and

$$\tau_{sp} = R_{sp} \, C \quad (14)$$

with R_{sp} the parallel equivalent resistance of R_s and R

$$R_{sp} = R_s \, R / (R_s + R) \quad (15)$$

Eq. 12a has been rewritten as Eq. 12b in order to obtain an expression which more clearly shows how dV_c / dt (written as a single term at the left side of $=$) depends on V_c (present as a single term at the right side) with a proportionality constant to be multiplied with V_c . Try to do the algebra of this rewriting yourself!

The meaning of differential Eq. 12b can now be investigated in the same way as for Eq. 5b for ERC-circuit I: V_c moves toward V_c^* , both from $V_c > V_c^*$ and from $V_c < V_c^*$, with a rate proportional to the absolute value of $V_c - V_c^*$ and inversely proportional to τ_{sp} , R_{sp} and C . At $V_c = V_c^*$ $dV_c / dt = 0$, then V_c^* (Eq. 13) is the value of V_c under **steady-state conditions**, as could have been found directly from Eq. 12a by filling in the steady-state condition $dV_c / dt = 0$. It depends on the relative value of R_s how close V_m^* is to E_s .

The **time behavior** of V_c , namely $V_c(t)$, can be found in the same way as for ERC-circuit I, i.e. by solving differential Eq. 12a (see PlenumBTOL). The result is given here directly:

$$V_c(t) = V_c^* + (V_c(0) - V_c^*) e^{-t / \tau_{sp}} \quad (16)$$

with V_c^* given by Eq. 13 and τ_{sp} given by Eqs. 14 and 15. Thus, the V_c transient is a single-exponential, moving from $V_c(0)$ to V_c^* with a time constant τ_{sp} determined by both R_s and R , but mainly by the smallest of the two resistors if they have a different value. One may be surprised that the time constant τ_{sp} is determined by the equivalent resistance R_{sp} of R_p and R in parallel, although the resistors are in series in the circuit. For the capacitor, they are apparently in parallel, because they are two parallel simultaneously charging/discharging pathways for the capacitor.

V_c^* in **voltage-clamp** ($R_s \ll R$) is unequal, though close to E_s , a condition different from that of V_c^* in ERC-circuit I. Thus, voltage-clamp of a leaky capacitor by the E_s / R_s source is never perfect. However, the equation for V_c^* (Eq. 13) shows that V_c^* can be very close to E_s , depending on the relative sizes of R and R_s . For $R \gg R_s$, voltage-clamp is very good, for example within 1% if $R > 100R_s$. Therefore, at very low R_s , both dynamic (small τ_{sp}) and steady-state (V_c^* close to E_s) voltage-clamp are good. The time course of V_c upon an E_s voltage-clamp step is graphically illustrated by Fig. 2.2b.

The **time course of the charging current** I_{rs} , $I_{rs}(t)$, now follows by substituting Eq. 16 in Eq. 1b. We have done something similar with ERC-circuit I, but the result is now different because of the presence of R:

$$I_{rs}(t) = [E_s - V_c(t)] / R_s \quad (17a)$$

or

$$I_{rs}(t) = [E_s - (V_c^* + (V_c(0) - V_c^*) e^{-t/\tau_{sp}})] / R_s \quad (17b)$$

with

$$I_{rs}(0) = [E_s - V_c(0)] / R_s \quad (17c)$$

and

$$I_{rs}^* = [E_s - V_c^*] / R_s = E_s / (R_s + R) \quad (17d)$$

The difference between Eq. 17 and the current equation of ERC-circuit I (Eq. 9) is that R allows a steady-state current to flow, namely I_{rs}^* .

Eqs. 13-17 allow us to further **define good voltage- and current-clamp conditions**. Eq. 13 implies that a leaky capacitor is very well voltage-clamped to the applied, E_s , if $R_s \ll R$. For that condition, Eq. 17 implies that the steady-state current in the circuit, I_{rs}^* , is then almost completely determined by R (or by conductance G, in Siemens, $S = 1/\text{Ohm}$) and that slow changes in R (or G) will be well reflected by I_{rs} changes. "Slow" means with transient times $\gg \tau_{sp}$, with $\tau_{sp} \sim R_s C$ ($R_s \ll R$). Voltage-clamp records are illustrated in Fig. 2.2b.

Good **current-clamp** conditions are guaranteed for the condition $R_s \gg R$, since then I_{rs} will be independent of R (cf. Eq. 17d).

V_c^* will then be (cf. eq. 13)

$$V_c^* = R I_{cc} \quad (18)$$

with the current-clamp current I_{cc}

$$I_{cc} = E_s / R_s \quad (19)$$

Although $I_{rs}(0)$ will still overshoot I_{rs}^* a little bit under this condition, the shape of the increase in current upon a step increase in E_s will be nearly stepwise. The time constant of $V_c(t)$ is now $\tau_{sp} \sim R.C$, which is much larger than under voltage-clamp with $\tau_{sp} \sim R_s C$. This is illustrated in Fig. 2.2c. Notice that the V_c value in current-clamp always remains a small fraction of the applied E_s !

2.3. Clamping an ERC model: ERC-circuit III

Cell membranes are leaky capacitors, which are charged because they accumulate charge on the capacitor through the "leaks" that generate a membrane potential. By voltage- or current-clamp stimulation one can change the charge on the capacitor. So far, we have neglected the presence of an **intrinsic voltage source in the leaky capacitor** stimulated by the external E_s/R_s source (ERC-circuit II). Fig. 2.3a shows ERC-circuit III, which is circuit II with the voltage source E placed as an extra component in the R branch, in series with R. Here we study the properties of this circuit,

which is equal to the WC-circuit drawn in Fig.1.2 for $R_s = R_{pc} + R_{pip} + R_{acc}$, $C_{pc} = C_{pip} = 0$. and for $R_{seal} \gg R$.

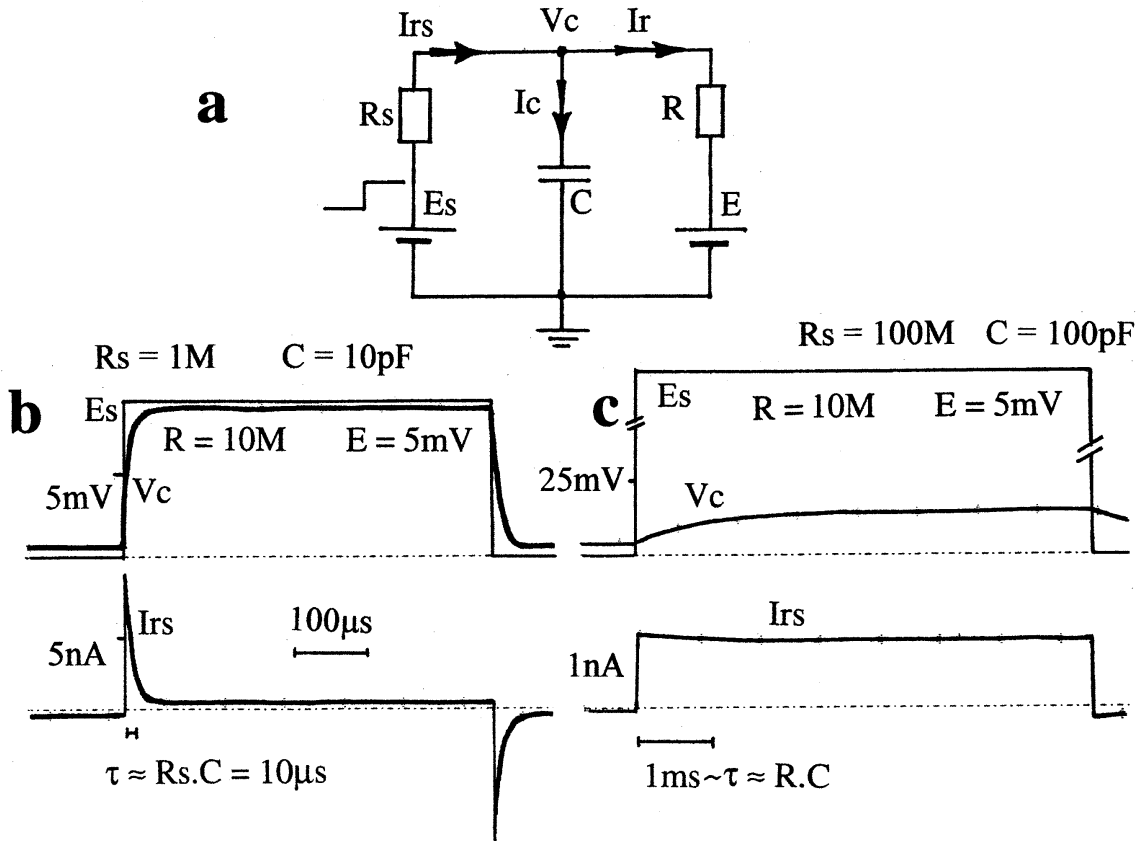


Figure 2.3. Clamping an ERC-model: ERC-circuit III. This circuit (a) contains, compared to ERC-circuit II, an extra voltage source E added in series with R . This makes the resulting ERC-circuit resembling a patch pipette with offset voltage or a cell membrane with membrane potential, voltage (b) or current (c) clamped by the E_s/R_s source. The E_s step in c is 100 mV. Note the difference in time scale between b and c. The records in b and c have been calculated for the indicated component values and are similar to those in Fig. 2.2b,c, except for the following differences: (1) E causes stationary (inward) current in b when $E_s = 0$ and the stationary current upon the E_s step is also different because of the presence of E ; (2) the V_c record in c now starts from E (here chosen positive) instead of from zero.

The behavior of ERC-circuit III upon steps in E_s can be derived in the same way as for ERC-circuit II. The only equation that is different is that for I_r , which is

$$I_r = (V_c - E) / R \quad (20)$$

This difference affects the differential equation resulting from the application of **Kirchoff's current law** to the currents in node V_c

$$I_{rs} = I_c + I_r \quad (21a)$$

which becomes, after substituting the equations for I_{rs} (Eq. 1b), I_c (Eq. 3) and I_r (Eq. 20),

$$(E_s - V_c) / R_s = C \, dV_c / dt + (V_c - E) / R \quad (22b)$$

The student herself may now derive all the other equations describing both the steady-state and dynamic behavior of ERC-circuit III upon steps in E_s by following the procedures explained under ERC-circuits 1 and 2. We provide them here without much further explanation of the derivations.

The rewritten **differential equation** is

$$dV_c / dt = -(1 / \tau_{sp}) \cdot (V_c - V_c^*) \quad (22c)$$

with

$$V_c^* = (R_s E + R E_s) / (R_s + R) \quad (23)$$

and

$$\tau_{sp} = R_{sp} C \quad (24)$$

with

$$R_{sp} = (R_s R) / (R_s + R) \quad (25)$$

The **steady-state behavior** of V_c , V_c^* , is given by Eq. 23. E is now present in the equation to contribute to V_c . The relative values of R_s and R determine whether V_c is more at the E_s side ($R_s \ll R$ for voltage-clamp by E_s) or at the E side ($R_s \gg R$ for current-clamp by the E_s/R_s source).

The **time behavior** of V_c upon steps in E_s is described by

$$V_c(t) = V_c^* + (V_c(0) - V_c^*) e^{-t/\tau_{sp}} \quad (26a)$$

with V_c^* given by Eq. 23. Note that Eq. 26a is identical to Eq. 16. The difference is in the actual value of V_c^* (Eq. 23) because of the presence of E . Upon **voltage-clamp** steps in E_s from $E_s = 0$ ($R_s \ll R$), V_c moves with a single-exponential time course ($\tau_{sp} \sim \tau_s = R_s C$) from a value close to the pre-step $E_s = 0$ value to one close to the E_s step value (Fig. 2.3b). Upon **current-clamp** steps in E_s from $E_s = 0$ ($R_s \gg R$), V_c moves relatively slowly (compared to under voltage-clamp) with a single-exponential time course ($\tau_{sp} \sim \tau_p = R.C$) from a value close to E to a value close to E plus a voltage drop across R due to the current-clamp current $I_{cc} = E_s/R_s$ (Fig. 2.3c). In equation

$$V_c(t) = E + R I_{cc} (1 - e^{-t/\tau_{sp}}) \quad (26b)$$

The equation for the **current behavior** of $I_{rs}(t)$ upon steps in E_s is obtained again by substituting Eq. 26a in Eq. 1b, which results in the next equation (the same expression as Eq. 17a):

$$I_{rs}(t) = [E_s - V_c(t)] / R_s \quad (27a)$$

or

$$I_{rs}(t) = [E_s - (V_c^* + (V_c(0) - V_c^*) e^{-t/\tau_{sp}})] / R_s \quad (27b)$$

with

$$I_{rs}(0) = [E_s - V_c(0)] / R_s \quad (27c)$$

and

$$I_{rs}^* = [E_s - V_c^*] / R_s = (E_s - E) / (R_s + R) \quad (27d)$$

Thus, E shows up in the expressions for the steady-state voltages and currents, whether they apply to voltage-clamp or current-clamp. In **voltage-clamp**, E does not contribute much to the clamped potential, but it does clearly contribute to the current, because E_s and E values in practical situations are of the same order of magnitude, while $R_s \ll R$ (cf. Eq. 27d). In **current-clamp** ($R_s \gg R$) E dominates V_c , but significant current to bring V_c away from E can only be applied if $E_s \gg E$. This is demonstrated by Eq. 23 after rewriting for the current-clamp (CC) condition $R_s \gg R$:

$$V_c^* = E + R I_{cc} \quad (28)$$

with

$$I_{cc} = E_s/R_s \quad (29)$$

Voltage-clamp and current-clamp records are illustrated in Fig. 2.3b and 2.3c, respectively. In principle they have the same shape, but the overshoot under current-clamp is hardly noticeable.

Instead of starting with the simpler circuits II and I, we could have started with ERC-circuit III for the derivation of all the equations describing the behavior of the circuit upon stimulation with voltage or current steps. We could have shown, then, that the equations for the simpler circuits II and I easily follow from those of the more complete ERC-circuit III. Assuming $E = 0$ yields the equations of circuit II, and assuming $E = 0$ and $R = \text{infinity}$ yields those of circuit I. The beginning student is better off with the above procedure, because the concepts and derivations are better introduced and explained there. The advanced student could, however, certainly follow the inverse sequence from circuit III to I.

The **general conclusion** from ERC-circuits I to III is that **voltage-clamp and current-clamp stimulation are extremes of the same stimulation technique** with an E_s/R_s -containing instrument. But membrane electrophysiologists know how different both techniques are in methodological respect and how important it is to have them both at your disposal. Good voltage-clamp allows complete voltage control over membrane conductance behavior, since the various ionic conductances in the membranes of living cells are voltage and time dependent but not current dependent. Thus, when applying constant current under current-clamp, the membrane voltage is changed. This may further amplify the changing voltage by opening up ionic channels affecting the membrane potential in the same direction and may result in an impulsive change in membrane potential called excitability. It was for the purpose of studying the mechanisms of excitability that voltage-clamp techniques were developed. Voltage-clamp instrumentation involves modern operational amplifier technology rather than a simple controllable E_s battery with a good low-resistance R_s component. Conceptually, however, the E_s/R_s combination serves as a good electrical equivalent of the clamp instrument because it summarizes what the technology has achieved: providing an ideal controllable voltage source with a relatively low output resistance R_s for the purpose of measuring very small currents (nA to pA).

2.4. Clamping an ERC cell membrane through a patch pipette: ERC-circuit IV

A cell membrane cannot directly be voltage- or current-clamped, as suggested by the discussions of ERC-models I-III. One always needs access electrodes between the clamping source and the clamped membrane. The **access pathway** directly connected to the cell is a patch pipette with its

narrow, high resistance tip and its pipette capacitance of the thin glass wall between the pipette solution and the extracellular bathing solution. The reference electrode usually does not add much access resistance or parallel capacitance to the circuit, because it is directly immersed in the bathing solution surrounding the cell (cf. Fig. 1.2). ERC-circuit IV in Fig. 2.4a gives a better representation of this condition than the previous circuits. It is identical to the circuit drawn in Fig. 1.2 for the WC-configuration (with $R_{\text{seal}} \gg R_m$). C_p and R_p may be seen as representing the pipette plus patch-clamp capacitance and the pipette plus access resistance, respectively, and C_m , R_m , and E_m represent the ERC-circuit of the cell. Usually, in voltage-clamp $R_s \ll R_p \ll R_m$ and $C_p < C_m$. If E_s is a step function, R_s acts as an access resistance for charging C_p . Subsequently, R_p acts as an access resistance to charge up C_m . Because there are two capacitors coupled by a resistor, there is a **two-phase charging process** in the measurement circuit, which occurs during each voltage-step in a patch-clamp experiment. This will be analyzed now using ERC-circuit IV.

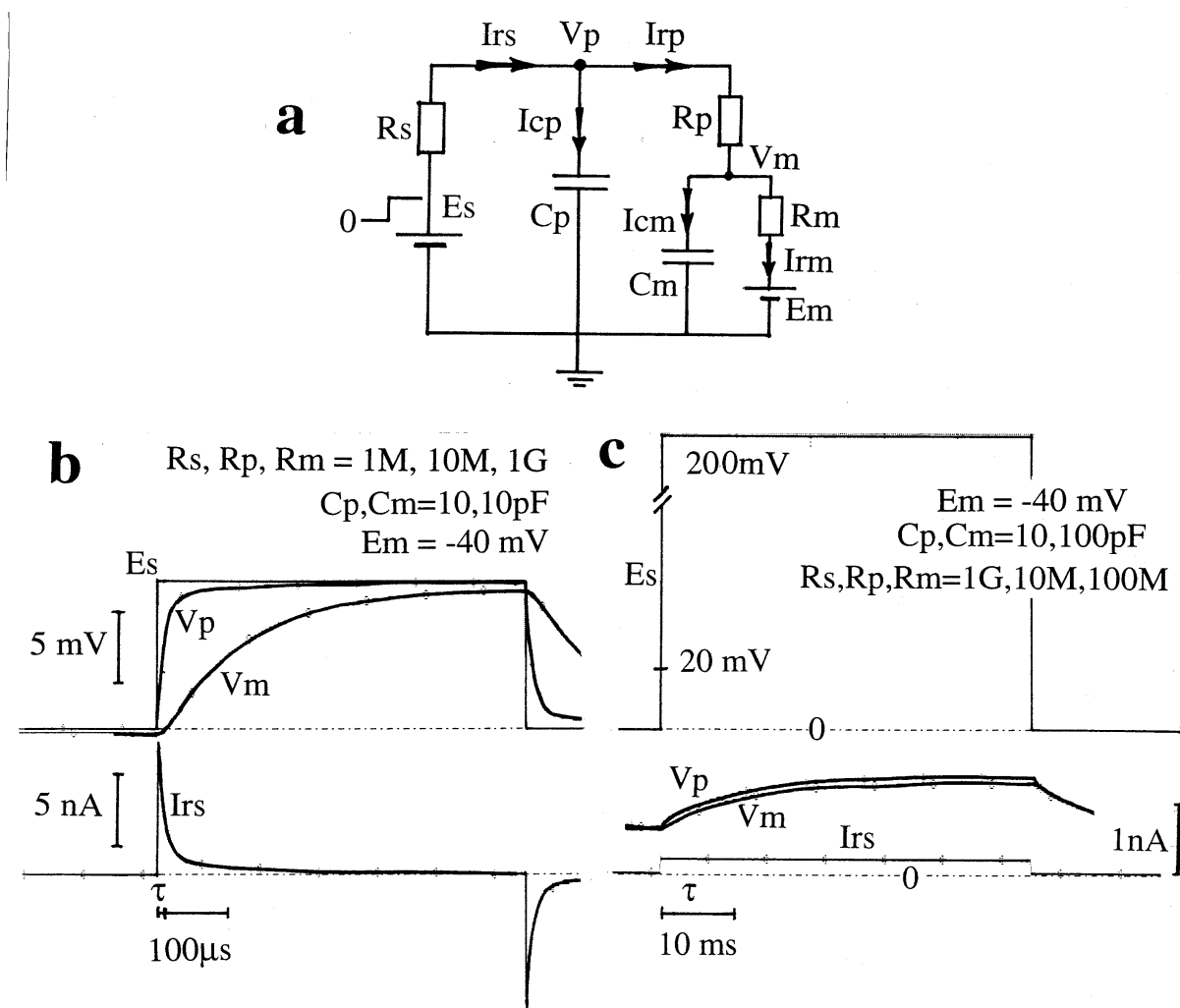


Figure 2.4. **Clamping an ERC cell membrane through a patch pipet: ERC circuit IV.** The circuit in a is Fig. 2.3a for a whole-cell configuration, extended with components representing the properties of the measuring patch pipet. The pipet resistance R_p is the access resistance to the $E_m/R_m/C_m$ membrane circuit, and C_p shunts the input of the E_s/R_s source. The presence of two capacitors (C_p and C_m) coupled by a resistor (R_p) makes the voltage-clamp (b) and current-clamp (c) responses biphasic (less clearly visible in current-clamp at the given resolution). Records calculated for the indicated component values.

After the discussion of ERC-circuits I to III, we don't need to explain the equations for currents through resistors (Ohm's law) or currents into capacitors (capacitor equation). We can instead directly apply **Kirchoff's current law** to the two nodes V_p and V_m .

For node V_p (see Fig. 2.4) we write

$$I_{rs} = I_{cp} + I_{rp} \quad (30)$$

or

$$(E_s - V_p) / R_s = C_p dV_p / dt + (V_p - V_m) / R_p \quad (31a)$$

or

$$R_s R_p C_p dV_p / dt = -(R_s + R_p) V_p + R_p E_s + R_s V_m \quad (31b)$$

Eqs. 31a is a first order differential equation, but its solution is undetermined because it includes V_m as another variable obeying another first order differential equation (see below). Given that V_m is undetermined, the steady-state solution of Eq. 31 (for $dV_p/dt = 0$) is

$$V_p^* = (R_p E_s + R_s V_m^*) / (R_p + R_s) \quad (32)$$

Although this equation does not provide a unique solution of V_p^* , because V_m^* is undetermined (V_m^* depends on E_m and R_m , which are not included in this equation, see below!), it provides a measure of V_p^*/V_m^* value pairs consistent with steady-state conditions. We need to incorporate E_m and R_m in the equation to find a unique value of V_p^* (see Eq. 36).

For node V_m (see Fig. 2.4a) Kirchoff's current law allows us to write

$$I_{rp} = I_{cm} + I_{rm} \quad (33)$$

or

$$(V_p - V_m) / R_p = C_m dV_m / dt + (V_m - E_m) / R_m \quad (34a)$$

or

$$R_p R_m C_m dV_m / dt = -(R_p + R_m) V_m + R_p E_m + R_m V_p \quad (34b)$$

Eq. 34b is also a first order differential equation. It is coupled to differential Eq. 31 through I_{rp} . Together these equations form a set of **two coupled linear first order differential equations**. The steady-state solution ($dV_m/dt = 0$) for V_m , again with no unique solution, is

$$V_m^* = (R_p E_m + R_m V_p^*) / (R_p + R_m) \quad (35)$$

Eqs. 32 and 35 form a set of two **steady-state equations** with two unknowns. We can solve them by substitution, both for V_p^* and for V_m^* . The result is

$$V_p^* = [(R_p + R_m) E_s + R_s E_m] / (R_s + R_p + R_m) \quad (36)$$

and

$$V_m^* = [R_m E_s + (R_s + R_p) E_m] / (R_s + R_p + R_m) \quad (37)$$

These equations imply that $V_m^* \sim V_p^* \sim E_s$ under good **voltage-clamp** conditions, with $R_m \gg R_p \gg R_s$, as wanted. However, V_p^* is closer to E_s than it is to V_m^* , because of loss of voltage across R_p . During practical experiments R_p (and an extra access resistance R_{acc} associated with R_p , see Fig. 1.2 and Chapter 3) may become a problem if R_m is not much larger than R_p . Then the cell will escape voltage-control and an excitable cell may fire a distorted action potential upon voltage-steps, seen as an action current instead of a voltage-controlled current.

R_p may also complicate **current-clamp** recordings, since V_p^* is usually measured instead of V_m^* , although the interest is in V_m^* . For the condition $R_s \gg R_m, R_p$ (current-clamp), Eq. 36 becomes

$$V_p^* = E_m + (R_m + R_p).I_{cc} \quad (38)$$

with

$$I_{cc} = E_s / R_s \quad (39)$$

Thus, only for $R_p \ll R_m$ the change in V_p^* upon current-clamp stimulation is largely due to R_m .

The **voltage time courses** $V_p(t)$ and $V_m(t)$ for E_s steps are more difficult to determine, because this requires solving two coupled differential equations. This can be done by writing first two separate second order differential equations by substitution of one into the other, and vice versa, as when solving any two equations with two unknowns. Both second order equations can be written in a general form

$$K_p.d^2V_p/dt^2 + L_p dV_p/dt + M_p V_p = N_p \quad (40)$$

and

$$K_m.d^2V_m/dt^2 + L_m. dV_m/dt + M_m V_m = N_m \quad (41)$$

with K, L, M and N being constants defined elsewhere (PlenumBTOL).

The solutions of these two equations have a general form (Hirsch and Smale, 1974; see Ince et al., 1986 for a similar problem).

$$V_p(t) = A_p e^{-t/T_{p1}} + B_p e^{-t/T_{p2}} + D_p \quad (42)$$

and

$$V_m(t) = A_m. e^{-t/T_{m1}} + B_m e^{-t/T_{m2}} + D_m \quad (43)$$

with A, B and D being constants. Thus, these solutions have the shape of the sum of two exponential functions, with T_1 and T_2 being complex functions of $\tau_{sp} = R_s C_p$, $\tau_{pm} = R_p C_m$ as well as other parameters.

Instead of analyzing the explicit expressions of Eqs. 42 and 43, here we follow a practical approach by numerically calculating the functions $V_p(t)$ and $V_m(t)$ for the equivalent circuit of Fig.2.4a under good **voltage-clamp** conditions ($R_s \ll R_p \ll R_m$). The forms of these functions are sketched in Fig. 2.4b. C_p is charged in two phases, an initial rapid phase and a second slow phase. C_m is charged with a sigmoidal time course in which the onset corresponds to the rapid charging of C_p and the later phase corresponds to the slow charging of C_p . The initial fast charge is close to the time constant $\tau_{sp} = R_s C_p$ and the long charge is close to the time constant $\tau_{pm} = R_p C_m$. Thus, the

time constants T1 and T2 in the equations Vp(t) and Vm(t) correspond to approximately to τ_{sp} and τ_{pm} , respectively. This seems reasonable because at extreme differences between Rs, Rp, and Rm, as occur during good voltage-clamp, charging of Cp and Cm is virtually independent. In the calculated **current-clamp** responses to Es steps, the presence of a significant Rp can be seen as an initial shoulder in the Vp(t) response and as a small delay in the Vm(t) response (see Fig. 2.4c). The calculated **charging currents, Irs(t)**, are also given in Fig. 2.4b,c. The voltage-clamp currents (lower record of figure b) clearly show successive Cp and Cm charging. Irs(t) was calculated from the equation (cf. Eq. 1b) :

$$I_{rs}(t) = (E_s - V_{cp}(t)) / R_s \quad (44)$$

The explicit form of this expression is not derived here.

For **voltage-clamp** conditions, the above equation describes what every patch-clamper knows well as a two-phase (fast and slow) capacitance charging current in response to voltage steps (see Fig. 2.4b), on which they spend so much time, cell after cell, to measure and cancel. The fast current transient mainly reflects Cp charging, while the slow transient mainly reflects Cm charging, as discussed above for the voltage changes Vp(t) and Vm(t).

Under **current-clamp** conditions ($R_s \gg R_p R_m$), Eq. 44 describes the current leaving the clamp instrument, but not exactly the current entering the membrane, because the initial fast current component mainly serves to charge Cp. The actual current of interest, I_{rp}(t), is described by

$$I_{rp}(t) = [(V_p(t) - V_m(t)) / R_p] \quad (45)$$

but it is impossible to catch this current in one-electrode patch-clamp experiments, in which one can only record current I_{rs} (in voltage-clamp) or V_p (in current-clamp). Fortunately, the difference between I_{rs} and I_{rp} is of no concern if $R_s \gg R_m \gg R_p$ and $C_p < C_m$. In that case the current steps are practically square both for I_{rs} and I_{rp}. There should nevertheless be a very small two-component overshoot in the applied current I_{rs}, but this is hardly visible in records (cf. Fig. 2.4c).

Eqs. 36, 37, and 42-44 are probably the most important and practical equations of this course, because they describe the patch-clamp stimulation technique in a way that includes both voltage- and current-clamp stimulation under ideal and non-ideal clamp-conditions. Although many problems can be understood through these equations, practical problems can, of course, be more complex than modeled by the ERC-circuits discussed so far. For example, a cell may be coupled to another cell or to surrounding cells (Harks et al, 200?) so that the stimulated object is no longer a single ERC-compartment. In that case the ERC-circuit representing the stimulated object should be extended with another resistively coupled ERC-compartment (Torres et al, 2004). If the equivalent circuit becomes complex, it may be useful to employ a computer model to simulate the measurement configuration or to make an electrical equivalent model as we did in Chapter 3 for demonstrating the ERC-circuit theory of this chapter (cf. Torres et al., 2004).

Finally, it is of interest to mention that ERC-circuit IV is identical to a **model of two electrically coupled cells**. The EsRsCp-circuit would represent cell 1 and the EmRmCm-circuit cell 2, with Rp being the coupling resistance of a gap junction. This model can be used to study the effect of Es

changes in cell 1 on V_m of cell 2, as well as the role of the membrane resistances (R_s , R_m), the coupling resistance (R_p), and membrane capacitors (C_p , C_m) in this interaction. Thus, ERC-models may be of great use, not only for practical patch clamping but also in more general problems of cell physiology.

2.5. Conclusion

A few final remarks may place the simple equivalent ERC-circuit approach of the present chapter in a broader perspective. This approach helps to understand how and what one is measuring during patch-clamping, but the **ERC-circuit theory used here only describes voltage and current changes upon abrupt changes of the components of the ERC-circuit**. Abrupt E-changes apply to the patch-clamp technique with its voltage- and current-clamp jumps. Abrupt R-changes apply to channel openings and closures and relatively sudden conductance changes. Sudden C-changes seem less relevant, but are nevertheless easily described with the same equivalent circuit theory. Fusion of two cells or vesicles with different membrane potentials would be an example of interest.

The simple **ERC-circuit approach does not apply to the kinetics** of voltage dependent channel or conductance activation, which is widely studied in membrane electrophysiology. This field of study requires additional concepts, bridging the microscopic mechanisms of single channel activation and macroscopic electric phenomena like excitability. Students interested in this subject are referred to the earlier chapters of the present book, to other texts (Hille, 2001) or are referred to the instructive teaching models now widely available (see PlenumBTOL).

A recommended next step after this chapter is to exercise your grasp of the equivalent circuit theory by testing it in a real patch-clamp set-up with a **model cell** displaying ERC-circuit properties like those shown above. How to proceed is explained in the next chapter. Or one could also directly go to actual patch-clamp experiments, but we have learned from experience that it is still difficult in the beginning to recognize ERC-circuit phenomena in living cells. Instant recognition during experiments may be important for quick decisions about how to continue successful protocols if technical problems arise. However, spending some extra time now on a model cell saves time in the long run, because the observations are not obscured then by accidental experimental complications.

3. MODEL CELL EXPERIMENTS.

3.1. Introduction

The following demonstrations and exercises will be presented more or less in the sequence of a real patch-clamp experiment, from switching on the equipment to, for example, pulling an outside-out patch, through all the intermediate phases, such as pipette testing, giga-sealing and whole-cell formation. Fortunately, this sequence is in line with the sequence of the ERC-circuits discussed in the previous chapter. We will often refer to those ERC-circuits, including the derived equations. No new equations need to be derived. The descriptions will be as if we were giving a demonstration, but with suggestions to the reader for doing her own extra experiments. If you do the experiments, make sure that you start each session with a standard amplifier and model setting (see below). Otherwise, you may get lost in abnormal amplifier behavior (e.g. oscillations), or the amplifier may look dead (in saturation), or you may misinterpret the model cell responses. Prevent touching the (+) input of the patch-clamp amplifier as much as possible, since your body is a capacitor (probably isolated from ground by non-conducting shoes) and may be charged to quite a few volts with respect to ground. This body capacitance tends to share its charge and voltage with the small input capacitance of the patch-clamp, and large voltages may damage the input. Therefore use insulated forceps to contact the circuit or ground yourself first before touching the circuit so that you will not carry large harmful voltages.

The importance of the demonstrations and experiments is that they provide **exercises in recognizing simple electric circuit behavior in complex experimental conditions**. Without such exercises it might take months, or even years, to develop that skill.

3.2. Model cell and measurement set-up description

3.2.1. Equivalent circuit

Fig. 3.1 shows the full electrical equivalent circuit of the model cell used to illustrate the electrophysiological properties of the various patch-clamp measurement configurations in a real patch-clamp set-up. It is an **ERC-circuit model**, i.e. it only consists of voltage sources (E), resistors (R) and capacitors (C). **Switches** (S1-12) are used at various points in the circuit to switch the circuit from one configuration to another or to represent opening and closing of ion channels and abrupt activation of ion conductances. It is very similar to the ERC-model in Fig. 1.2b but more detailed. For example, it includes specific resistors or conductors in the CAP and WC and also allows the establishment of the IOP, OOP and ppWC configuration. E, R and C components and values as well as switches are listed in Table 3.1. Component values are in the physiological range. Switches are drawn in the standard initial positions, from where changes are defined.

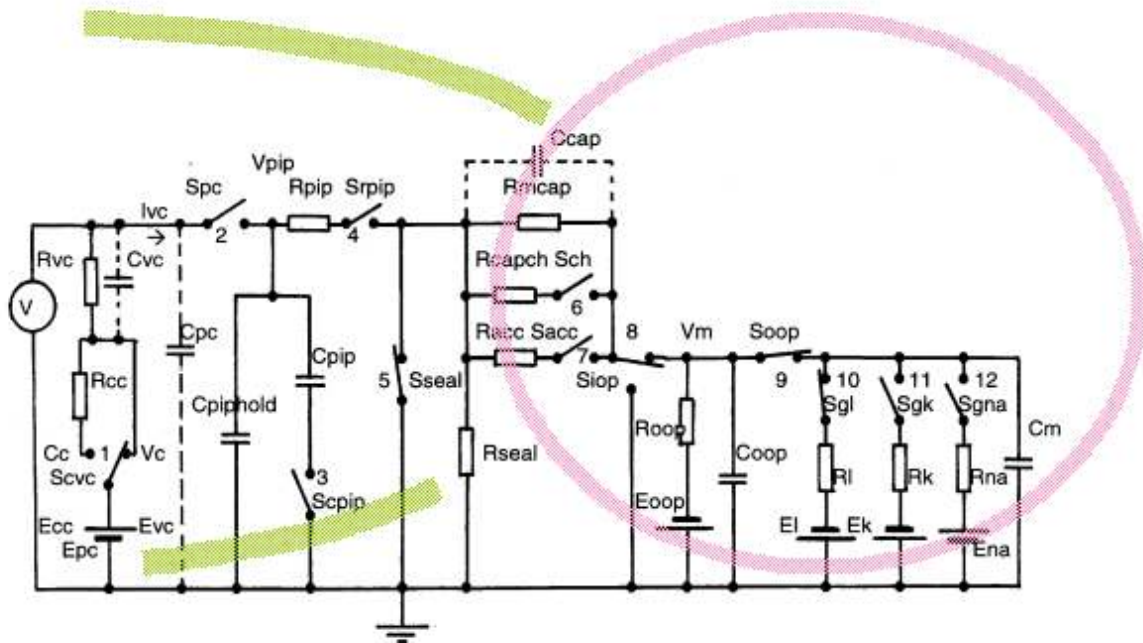


Figure 3.1. Diagram of the electrical equivalent circuit of the model used to exercise patch-clamp procedures and measurements. The dashed capacitors are stray capacitances, not added to the circuit as components. A schematic drawing of the measurement configuration (pipette tip left, cell right) has been overlaid over the circuit to identify the physical and biological origin of the circuit components. For further explanations, see text and for component values, see Table 3.1.

The circuit left of the patch-clamp connection switch S_{pc} (# 2) is the **ERC-circuit equivalent of the patch-clamp amplifier**. Switch S_{vc} (# 1) is used to switch between the two measurement modes, voltage-clamp (vc) and current-clamp (cc). The circuit includes an ideal volt (V) meter and an ideal current (I) meter (with $I = V_{vc}/R_{vc}$ representing the current to voltage conversion). E_{pc} corresponds to E_s , and R_{vc} and R_{cc} represent the two extremes ($R_{cc} \gg R_{vc}$) of R_s values in the ERC-circuits of the previous chapter. C_{pc} is the input capacity of the patch-clamp. Switch S_{pc} connects the pipette-holder (with pipette) to the patch-clamp and introduces the extra capacity $C_{piphold}$ to the amplifier input. Practical information on patch-clamp amplifier settings is given below. Simultaneous closing of switches S_{cpip} (# 3) and S_{rpip} (# 4) represents **entering the bath solution with the pipette**, thus connecting pipette capacitance C_{pip} and pipette resistance R_{pip} to the patch-clamp input. Closing only S_{cpip} simulates testing a clogged pipette with immeasurably high R_{pip} . Opening switch S_{seal} (# 5) after closing switches 2, 3, and 4 symbolizes **giga-sealing** of the pipette tip to the cell and the **formation of a cell-attached patch (CAP)** with resistance R_{cap} and capacitance C_{cap} . Closure of channel switch S_{capch} (# 6) in the CAP activates a CAP-channel by inserting in the CAP the CAP-channel resistance R_{capch} , shunting the resistance of the CAP membrane, R_{mcap} . R_{cap} is the equivalent of R_{mcap} and R_{capch} in parallel. The CAP-membrane and CAP-channel have not been given intrinsic voltage sources (CAP-membrane potential and channel reversal potential), assuming that the pipette solution has an ionic composition, which is essentially the same as the cytoplasm.

Breaking the CAP for **establishing the whole-cell (WC)** configuration is simulated by closing access switch Sacc (# 7), which short-circuits Rcap by inserting the much lower access resistance Racc as an extra resistance in series with Rpip. Switching inside-out-patch (IOP) switch Siop (# 8) to the left, from its WC-position to the IOP-position while Sacc is open, imitates **excision of an IOP** from the cell by abruptly pulling up the pipette in the CAP-configuration. With Sacc closed, Siop in the WC-position and outside-out-patch switch Soop (# 9) closed we are in the conventional WC-configuration, from where we can **enter the OOP-configuration** by opening switch Soop. Conductance switches Sgl (# 10), Sgk (# 11) and Sgna (# 12) can be used to suddenly activate or deactivate the three WC membrane conductances Gl (leak conductance), Gk (K⁺ conductance) and Gna (Na⁺ conductance), respectively. Total membrane conductance $G_m = G_m' + G_{oop}$, with G_m' being the sum of the active conductances Gl, Gk, and Gna, thus excluding G_{oop} and G_{cap} . WC membrane capacitance is $C_m = C_m' + C_{oop}$, thus excluding C_{cap} . **Formation of the permeabilized-patch WC (ppWC)** configuration is simulated by inserting successively decreasing Racc values

The grounded side of the circuit is the extracellular side of the cell membrane. The patch-clamp potential, Epc, the pipette potential, Vpip, the membrane potential, Vm, and the reversal potentials, Eoop, El, Ek, and Ena are measured (or defined) with respect to this extracellular ground potential. Vrv is the voltage across the resistor Rvc.

3.2.2. Model hardware

The present information on the hardware components and patch-clamp set-up that we used is only important for those students who want to do the model exercises themselves in their own time on an available patch-clamp set-up. The other students can directly proceed to the demonstrations (Chapter 3.3.).

The **model circuit** was not constructed by soldering together ERC components and mechanical switches. That turned out to be unsatisfactory, because of unwanted stray capacities in the switches, sensitivity to hand-movement artifacts during manipulations on the circuit, and limited flexibility for changes of the circuit. Furthermore, switches showed “bouncing” of the contacts causing undefined switching. We preferred to employ commercially available circuit boards ("bread boards") generally used for prototype circuit building and for teaching. A small board of 8x6cm (see Fig. 3.2) was ideal to build up the entire circuit and to place it on the stage of the microscope instead of a cell chamber with bathing solution and cells. It was fixed in place with magnetic strips adhering to a grounded metal plate on the microscope stage. This plate in fact corresponds to the grounded bath solution around the cells in a cell chamber. Working in this way and using the regular equipment of a set-up gives the "feel" of doing a real patch-clamp experiment. One also benefits from the grounded environment around the model circuit, screening off the model cell from 60 (or 50) Hz interference.

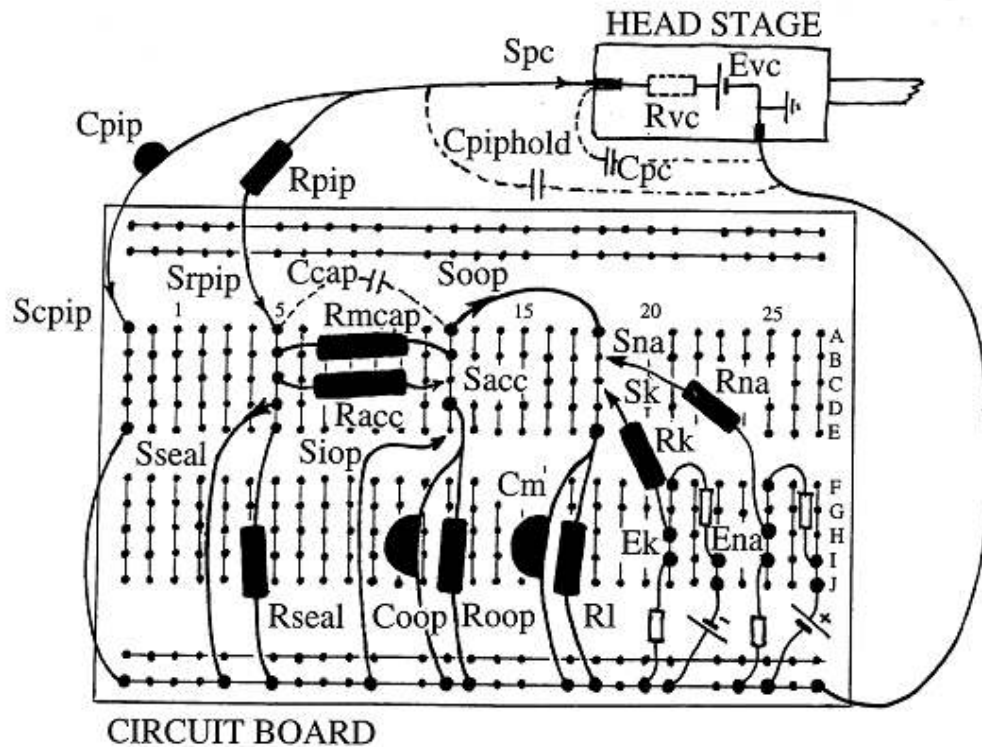


Figure 3.2. Example of equivalent circuit wiring on the breadboard (or circuit board). The figure shows a 8x6cm breadboard seen from above. The dots are wire insertion holes for easily making electrical connections without soldering. The straight lines between the dots are the connecting wires between the insertion holes, under the surface of the board. These connections cannot be seen but can be checked with an Ohmmeter. By inserting the leads of the components (resistors, capacitors, batteries) in the holes, one can easily build circuits to study the electrical properties of the various patch-clamp configurations and to exercise the experimental procedures. Resistors (cylinders) and capacities (half-drops) added as components to obtain the equivalent circuit of Fig. 3.1 are black. The switches of the circuit diagram in Fig. 3.1 are just the leads with the arrow points, pointing to or from a connection hole. The enlarged dots show the established contacts. Arrows pointing to close-by holes indicate switch contacts to be made during the proposed series of model experiments. Arrows pointing away from holes indicate contacts to break during the experiments. By comparing this practical breadboard circuit with the circuit diagram in Fig. 3.1, one can identify the various components. In the present circuit wiring, the probe (pre-amplifier) of the patch-clamp amplifier has been connected to the pipette-holder with pipette (switch S_{pc} on), the “pipette has entered the bathing solution around the cell” (S_{cpip} and S_{srpip} on) and the pipette is “touching the cell, ready for giga-sealing”. Giga-sealing is established by opening the seal switch, S_{seal}. This results in the CAP measurement configuration. By connecting R_{acc} to hole 12C (switch S_{sacc} on), one can make a WC from the CAP. By opening S_{soop} one obtains an OOP from the WC. In stead, connecting S_{siop} under CAP conditions results in an IOP. With switches S_{sk} and S_{sna} one can introduce into the WC a G_k and a G_{na}, respectively. The Nernst potentials have been established with a simple voltage-divider circuit (the small white resistors). The leak conductance and the OOP conductance has been given in this figure a reversal potential of 0mV. The interrupted-line wires are non-existing wires, but indicate the presence of stray capacities (C_{pc}, C_{piphold}, C_{cap}). Resistor R_{capch} with switch S_{capch} (Fig. 3.1) is not shown on the circuit board

A **breadboard** is a plastic board with groups of rows of internally interconnected holes for insertion of the leads of the components (Fig. 3.2). Connected holes quickly join components together (instead of soldering) and unconnected rows of holes can be bridged by components, thus easily creating ERC-circuits of a pipette, a membrane patch, and a whole-cell membrane as well as the switches between these circuits and the components. The switches were just simple solid (insulated) wires (Sseal, Siop, Soop), or component leads, inserted into or pulled out of the holes by hand or by using a forceps with insulated tips. In certain cases, when switching had to occur quickly and be well timed, magnetic switches (reed contacts) were used. Moving a small magnet on a rod along the contact operated magnetic switches. In order to protect the input of the amplifier during manipulation, we insulated the leads of components by putting shrink isolation tubing around them. This tubing shrinks tightly around the leads when heated, for example, by holding a solder gun close to the tubing.

Small-size 3.4-volt lithium cells in a voltage-dividing resistor circuit were employed to obtain physiological reversal potentials for insertion in the parallel conductance branches of the cell membrane. Resistor values of 1-100 M Ω and capacitors of 1-100pF can usually be obtained in a departmental electronic workshop or can be bought in a commercial shop for electronic components. Higher resistor values probably need special ordering. Axon Instruments Inc. (Foster City, CA 94404, USA) offers a low-price selection of Giga Ohm values. Low stray capacity (< 0.5pF) is an important specification of good high resistance components, in particular for the cell-attached-patch resistors and the seal resistance. The small capacity Ccap was not an added component, but was the actual stray capacitance naturally associated with the circuit connections in the board and with the resistors coupled together in the CAP-section of the model.

3.2.3. Patch-clamp set-up

Each **patch-clamp set-up** requires specific instruction. Therefore, we only briefly describe the patch-clamp set-up we used for the demonstration measurements presented here. The heart of the set-up is the cell chamber on the stage of the microscope with the small patch-clamp preamplifier box (probe or head-stage) above the cells. The head-stage is held and manipulated by a micromanipulator and has a connector for connecting the pipette-holder. In our exercises the circuit board with **the cell model takes the place of the cell chamber**, and a 5-cm wire serves as a pipette-holder connecting the (+) input to the pipette resistor, Rpip, and pipette capacity, Cpip (Fig. 3.2). The grounded reference (-) input of the head-stage (the probe) is connected to the external side of the model membrane. The patch-clamp used is the **L/M-PC amplifier** of List-Medical (D-6100 Darmstadt, Germany). As all commercial patch-clamps, it can either be used in the voltage-clamp or current-clamp mode. It also has the standard facility to cancel fast (pipette) and slow (whole-cell) capacitance currents and to measure the capacities (Cpip and Cm) and series resistances (Rvc and Rpip + Raccess) causing these voltage-step induced transients. The amplifier is equipped with electronic low-(frequency)-pass filters to remove high-frequency components from the signal at different cut-off frequencies (1-80KHz).

It is important that all switches and dials of the main patch-clamp unit in the rack are in **standard initial positions** before starting any experiment: Amplifier mode should be on voltage-clamp; Vpip

offset and Vhold potentiometer dials should be on zero; series compensation should be off; capacity cancellation dials should be on zero, and the cancellation switch(es) should be off; filter setting should be on 10 kHz (80 kHz in the initial experiments, see Fig. 3.3), and step steepness on 2 μ s rise time (no rounded voltage steps). Finally, the gain and stimulus scaling should be standard or as required by the software used.

The application of **voltage- and current-clamp protocols** to the model cell and the simultaneous storage of the evoked responses can be controlled by a personal computer using **pClamp/Clampex** software of Axon Instruments (Foster City, CA 94404, USA). The monitor of the PC run by pClamp can in principle be used as an oscilloscope screen to monitor the stimulus steps and the current or voltage responses, but we found it useful to use a separate oscilloscope and simple block pulse generator for extra tests. Emphasis in this demonstration is on the direct interpretation of the records, so we will not use sophisticated data analysis procedures. Note that pClamp is not necessary for these experiments; all that is required is a function generator and an oscilloscope.

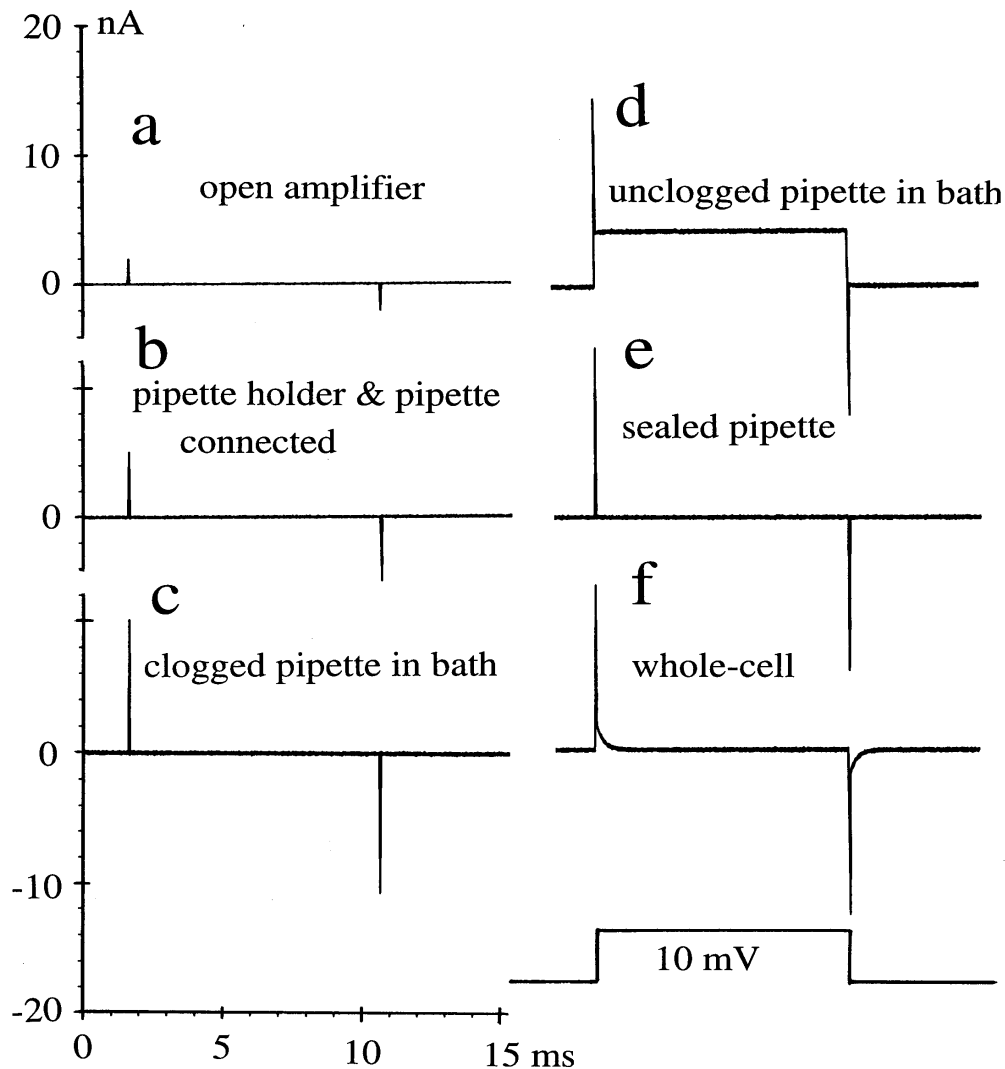


Figure 3.3. Voltage-clamp records obtained during patch-clamp procedures leading to the whole-cell (WC) configuration, all on one scale (lowest gain recording). The various procedures, described in the text, were carried out while applying voltage-clamp steps of 10mV. The initial model settings were as illustrated in Fig.3.1. Record **a** applies to these initial settings. Record **b** is taken after closure of switch S_{pc}, **c** after closing S_{cpip}, **d** after closing S_{rpip}, **e** after opening S_{seal} and **f** after closing S_{acc}. The model components were as in Table 3.1, with R_{acc}=2.2M, E_l=E_{oop}=~-60mV. The G_k and G_{na} branches were not connected (switches 10-12 open). Amplifier settings: 80KHz filtering and no capacitive transient cancellation.

3.3. Patch-clamp measurement procedures and configurations

3.3.1. Switching-on the patch-clamp: amplifier open input capacitance and resistance, and filtering

When you observe a patch-clamp experiment for the first time, you may see the patch-clamper turning on her equipment and bringing the switches and dials of her patch-clamp and other instruments to standard settings. Then she may start **voltage-clamp step stimulation** while watching the oscilloscope for the display of signals. The voltage steps clearly evoke sharply

peaked, needle-like current responses ($\sim 30\mu\text{s}$ **spikes** at 10KHz low pass filtering; $\sim 5\mu\text{s}$ spikes at 80KHz filtering, see Fig. 3.3a). But, what is being clamped here? There is no pipette or cell connected to the input. The input is open. It is only exposed to the air! Is the air being voltage clamped? In a sense, yes.

That there is no steady current during the application of steady voltage is no surprise, since air has no conductance (infinitely large resistance). But then, where do the spikes come from? Although air has no conductance, it separates the conducting input terminals. And one of these, the (-) input (the reference electrode) is connected to ground, i.e. to a great conducting mass surrounding the set-up, and therefore in some proximity to the (+) input (the measuring terminal). Thus, air functions as a dielectric, creating capacitance which is called here **stray capacitance** (C_{str}), because it is unintended and distributed (strayed) over the conducting mass around the (+) input terminal, inside and outside the head-stage in an unforeseeable way, but clearly measurable. It is this capacitance, also indicated as C_{pc} (C of the patch-clamp), which is charged by the voltage-clamp step through the internal resistance R_{vc} of the amplifier (Figs. 3.1 and 3.2). And the resulting short-duration charging currents, spike-like on a ms-time base, are visible on the oscilloscope. Note that this is an example of ERC-circuit I (Fig. 2.1)! The appearance of the spikes on the oscilloscope indicates to the experimenter that the patch-clamp amplifier and connected equipment are working and that she may go on to the next step in her experiment.

But first we measure this stray capacity C_{pc} . The patch-clamp instrument is equipped with a capacity measurement option based on precise **cancellation of a capacitance current transient** by adding to the transient at the input (from within the amplifier) an identical (single-exponential) current transient of opposite polarity. At precise cancellation the adjustment dials can be read off in terms of canceling capacitance C_{f} (f of fast transient) and canceling time constant τ_{f} or resistance R_{f} (or conductance G_{f}). R_{f} can be derived from τ_{f} and C_{f} or τ_{f} can be derived from R_{f} and C_{f} using $\tau_{\text{f}} = R_{\text{f}} C_{\text{f}}$, as explained at ERC-circuit 1. With this cancellation measurement, which can be carried out at any filter setting though easier at the higher settings, we find for our patch-clamp that $C_{\text{f}} = C_{\text{pc}} = 1.0 \text{ pF}$ at $\tau_{\text{f}} \sim 2 \mu\text{s}$. This capacitance may look very small, but is nevertheless well measurable. The time constant τ_{s} could not precisely be determined from the dial, but the estimated C_{f} and τ_{f} values allow us to calculate an estimated series resistance $R_{\text{vc}} = R_{\text{f}}$ from $\tau_{\text{f}} = R_{\text{vc}} C_{\text{pc}}$ (cf. ERC-circuit I). Then, R_{vc} seems to be $\sim 2\text{M}\Omega$. This is too large for reliable voltage-clamp measurements of $R_{\text{pip}} \sim 1\text{M}\Omega$, as we will see below. What could be the reason of this high estimated R_{vc} value? It may be an inaccurate reading of the τ_{f} canceling dial. This dial is not well calibrated, because measuring τ_{f} is not an important goal during patch-clamp experiments.

Let us try to obtain R_{vc} from direct, **current peak measurements**. At ERC-circuit 1 it was explained that $R_{\text{vc}} = dE_{\text{vc}}/dI_{\text{peak}}$. Therefore we measure dI_{peak} at 10KHz (standard) filtering for E_{vc} steps of 10mV and use this equation. We find $R_{\text{vc}} = 10\text{mV}/0.5\text{nA} = 20\text{M}\Omega$. Even much higher than the value obtained by the canceling procedure! What could be the reason here for the overestimation of R_{vc} ? One possible answer is the internal filtering in the patch-clamp amplifier, which lowers dI_{peak} .

We do not discuss here signal **filtering** in terms of ERC-circuits. The relationship between RC-filtering and frequency filtering is further explained in PlenumBTOL. Filtering is here simply defined as an electronic procedure to selectively suppress fast wave (high frequency), medium or

slow wave (low frequency) components of a recorded signal such as a voltage-clamp current signal. A patch-clamp usually has various filter settings allowing to remove the higher frequency components from the record. Standard filter setting used here is at a cut-off of $>10\text{KHz}$ frequencies. This means that the $30\text{-}\mu\text{s}$ duration transient is a drastically filtered signal, due to a frequency setting that is too low to faithfully record the fast capacitance peak transient. This results in a drastic reduction of the peak amplitude of the fast capacitance current transient and in a much slower time course of the remaining $30\text{-}\mu\text{s}$ signal.

This is a reason to record the fast transient at the best possible frequency setting: 80KHz (as in Fig. 3.3). This high frequency filter requires recording at a better time resolution than the analog-to-digital conversion (ADC) card for pClamp controlled data storage may provide. Therefore, the readings are done from the oscilloscope. We find shorter ($\sim 5\mu\text{s}$) and much higher peak transients ($\sim 2.6\text{nA}$ on the scope, $\sim 2\text{nA}$ in pClamp records, see Fig. 3.3a) and, consequently a much better R_{vc} value ($\sim 4\text{M}$), but still worse than the amplifier rating. Understandably, we cannot reliably measure a $5\text{-}\mu\text{s}$ transient with an 80KHz filter. Furthermore, the steepness of the voltage step ($2\mu\text{s}$) also limits I_{peak} of the presumed $5\text{-}\mu\text{s}$ transient. Thus we may think that measured I_{peak} values are too low and, consequently, calculated R_{vc} values too high. As we cannot do better now, we find another way to estimate R_{vc} below.

We summarize the results and **conclusions** as follows:

- * Although the charging current transients upon voltage steps are heavily filtered by the amplifier, current cancellation is perfectly possible with fast ($\tau \sim 2\mu\text{s}$) single-exponential current transients of opposite polarity.
- * Thus, ERC-circuit I applies to the open input properties of the patch-clamp amplifier, and, in principle, it is possible to measure input capacity and resistance by cancellation.
- * Series resistance (R_{vc}) estimation from current peak measurements provides R_{vc} values that are too high because of signal filtering inside the amplifier.

3.3.2. Connecting the pipette-holder with pipette to the patch-clamp: extra stray capacity

We expect that connecting the pipette-holder (with inserted pipette) with its stray capacity (C_{str}) to the input would affect these spikes by making them wider, but not higher, as we predicted from the properties of ERC-circuit I. This is because the mass and surface of the input wiring is increased, and probably also the proximity to ground. If the charging source voltage-step E_{vc} and the charging internal source resistor R_{vc} remain the same and C_{str} increases, then the charging time constant would increase but not the peak height of the charging current. This can be checked by **connecting a pipette-holder (with inserted pipette) equivalent** to the (+) input by closing switch S_{pc} (see Figs. 3.1 and 3.2), namely, a 5cm wire, a soldered resistor, $R_{\text{pip}}=2.2\text{M}$, and a capacitor $C_{\text{pip}}=4.7\text{pF}$ (not grounded). All other switches of the circuit are in the initial standard setting; filter still at $>80\text{KHz}$ cut-off). Maybe to your surprise, it is the peak of the spike that is increased rather than the spike duration (cf. Fig. 3.3a,b). The added capacitance, measured by cancellation at $\tau_f \sim 2.5\mu\text{s}$ (for best canceling), is $\sim 1.0\text{pF}$.

What is the cause of the **increase in peak height instead of peak width** when increasing C ? The answer, which again lies in the internal filtering of the amplifier, will also solve the above problem

about why the R_{vc} values calculated from the peaks of the fast capacitance transients are too high. We don't touch this problem here, because it is not of great importance for actual patch-clamp experiments on living cells. We just mention here that we have to consider a stray capacity C_{vc} across R_{vc} to explain the increase of peak width with C . A detailed explanation is given in PlenumBTOL.

Assuming this rather difficult to understand filtering effect of C_{vc} , we further explore the effect of externally added stray capacity on the fast capacitance current (I_{cf}) transient by inserting a longer (10-20cm) wire (unconnected to the reference input terminal) in the (+) input. Indeed, we do see now an even further increased C_{str} (measured by cancellation). We can also observe an increase in C_{str} when the wire is brought closer to surrounding grounded objects. Wires of the type used by us introduce approximately **$C_{str} \sim 0.1\text{pF per } 2\text{ cm wire length}$** . The same wire in the reference input does not have effect, unless the wire is used to bring ground closer to the (+) input. Apparently, the surface enlargement of the already large ground mass does not contribute to C_{str} . C_{str} can be increased drastically by holding the (insulated!) input connection wire (pipette-holder) between your fingers and grounding yourself, because this action brings ground very close (but not in touch!) to the (+) input terminal!

These simple tests illustrate not only the drastic effects of stray capacity, but also indicate an obvious way to obtain better estimations of R_{vc} . This is done by measuring capacitance peak height at higher and higher C 's intentionally applied across the patch-clamp input, and by calculating the R_{vc} values from dE_{vc}/dI_{peak} until calculated R_{vc} becomes constant. In this way one can find that **$R_{vc} < 100\text{Kohm}$** , quite acceptable for a patch-clamp which should be able to measure R_{pip} values $>1\text{M}\Omega$.

During these measurements with increasing C 's one only observes slower capacitance transients with increasing C 's for the higher C 's (equal to or $>C_{vc}$), because the time constant of the transients is $R_{vc} \cdot (C_{vc} + C_{external})$, as explained above. But the shapes of these transients, in particular at small applied C 's, are not pure single exponentials but show "**oscillatory ringing**", i.e. over- and under-shoot behavior upon voltage-step stimulation. This response too abrupt stimulation stems from the properties of the filters of the amplifier and makes it difficult to recognize the single-exponential nature of the fast capacitance transients. The fact that these fast capacitance transients are very well cancelable by single-exponential transients of opposite polarity at the input means that the $E_{vc}/R_{vc}/C_{pc}$ ERC-circuit of the patch-clamp still holds and that the non-exponential shape of these fast transients are **response deformations resulting from amplifier (filter) properties**. However, these deformations do affect capacitance peak current measurements. Thus, calculated R_{vc} values are not precise but can be improved by using less steep voltage steps causing less ringing. (Try it, this option is present on the patch-clamp). Nevertheless, the drastic increase in ΔI_{peak} with increasing applied C shows that calculated R_{vc} values are orders of magnitude smaller than measured at the intrinsic $C_{pc} = 1\text{pF}$. For precise R_{vc} measurements we would need another approach (not discussed here).

Sooner or later you may switch the patch-clamp to **current-clamp** while measuring in the air. Do it now to discover that the voltage is probably not stable at 0 V but soon increases to large (out of range) positive or negative values, even though there is no voltage source connected to the input or intentional current injected into the input. The reason of the building input voltage is a tiny **offset**

current produced by the amplifier input and injected into the stray capacity at the input from inside. Thus, the accumulating charge on C_{str} causes the increasing potential, as explained at ERC-circuit I and illustrated in Fig. 2.1c. Switching the amplifier back to zero voltage-clamp can easily discharge the input again.

The CC_{zero} screw on the front plate of the L/M-PC patch-clamp can compensate the input offset current. It will be very difficult to zero the input potential at an open input, but you can show that bringing offset compensation out of balance in the positive or negative direction determines the polarity and the speed of input voltage development. This **input offset current compensation** procedure is of great importance for voltage measurements from high-resistance voltage sources, as we will see later.

We draw the following **conclusions** from these experiments:

- * Stray capacity, amplifier filtering, and input offset current further complicated our open-input patch-clamp measurements to identify ERC-circuit I in this measurement condition.
- * The tests on stray capacity showed that two factors are of importance to reduce C_{str} , one is the size of the leads to the (+) input, the second is the proximity of these leads to ground surfaces. This is, for example, important in the design of pipette-holders (Buisman et al, 1990), which should not add more than 0.5pF to the input capacitance of the patch-clamp.
- * Adding capacity to the patch-clamp amplifier input was a useful method to estimate the value of R_{vc} and the series resistance in charging C_{str} , according to equivalent ERC-circuit I.
- * Amplifier filtering deformed the capacitance current responses to steep voltage steps, but this deformation did not affect the capacity measurements by cancellation.
- * Input offset current errors in voltage measurements are important to consider when measuring from high-resistance voltage sources.

3.3.3. Immersing the pipette to measure pipette capacitance and resistance

We proceed with the patch-clamp experiment by "immersing the pipette tip in the bathing solution" (by closing switch Sc_{pip} in Fig. 3.1) during **voltage-clamp stimulation** to find out that "the pipette tip is not well filled with pipette solution and is clogged by an air bubble in the outer tip" (S_{pip} is not yet closed, see Fig. 3.3c). This allows us to observe the effect of **inserting only C_{pip}** in the circuit without masking the charging current I_{cpip} by the current through the pipette resistance R_{pip} . We see again an increased spike peak (cf. Fig. 3b and 3c) rather than increased spike duration. C_{pip} measurement by cancellation yields $C_{pip} = 5\text{pF}$ (nominal value 4.7pF) as an added capacitance to $C_{pc} + C_{piphold}$ (~2pF). Cancellation this increased C_f value requires an increased τf value, as expected from $\tau = R.C$.

C_{pip} is the capacitance between the pipette solution and the bath solution across the thin glass wall separating the two conductors. We are clamping the glass wall of the non-conducting pipette! In practice one can check that this immersed glass wall is the origin of C_{pip} by immersing the pipette deeper into the solution. It will increase C_{pip} .

Now it is time to "unclog the pipette by removing the air bubble by suction or blowing". If that is unsuccessful, we "take a pipette that is filled better." Both actions correspond to **inserting R_{pip}** by closing switch S_{rip} in addition to switch S_{cpi} (switch #4 in Fig. 3.1). The voltage-clamp step now causes steady (DC) current to flow during the pulse after the initial I_{cf} spike (Fig. 3.3d). The applied voltage divided by the measured steady current yields a resistance of $2.2M\Omega$, which is the right value. Thus, the voltage-clamp is good enough to reliably measure $R_{pip} \sim 2M\Omega$, which implies that $R_{vc} \ll 2M\Omega$.

The spiky, cancelable, and overshoot current response to the voltage step indicates that the immersed pipette has the properties of ERC circuit II, even though this spike is strongly affected by amplifier filtering, as explained above for the role of C_v in this filtering. Therefore, this spike can only be seen clearly when the amplifier is set at sufficiently high (80KHz) low-pass filtering, because the spike is a high frequency signal. At lower high frequency cutoffs (e.g. 10KHz) the spike may become lower than the steady current response of a pipette, in particular when $R_{pip} < 2M\Omega$. Fig. 3.4a is a record example, where the spike just overshoots the steady pipette current at 10KHz filtering. When using PC controlled analogue-to-digital conversion (ADC) one may miss such fast transients when choosing too low sample frequencies.

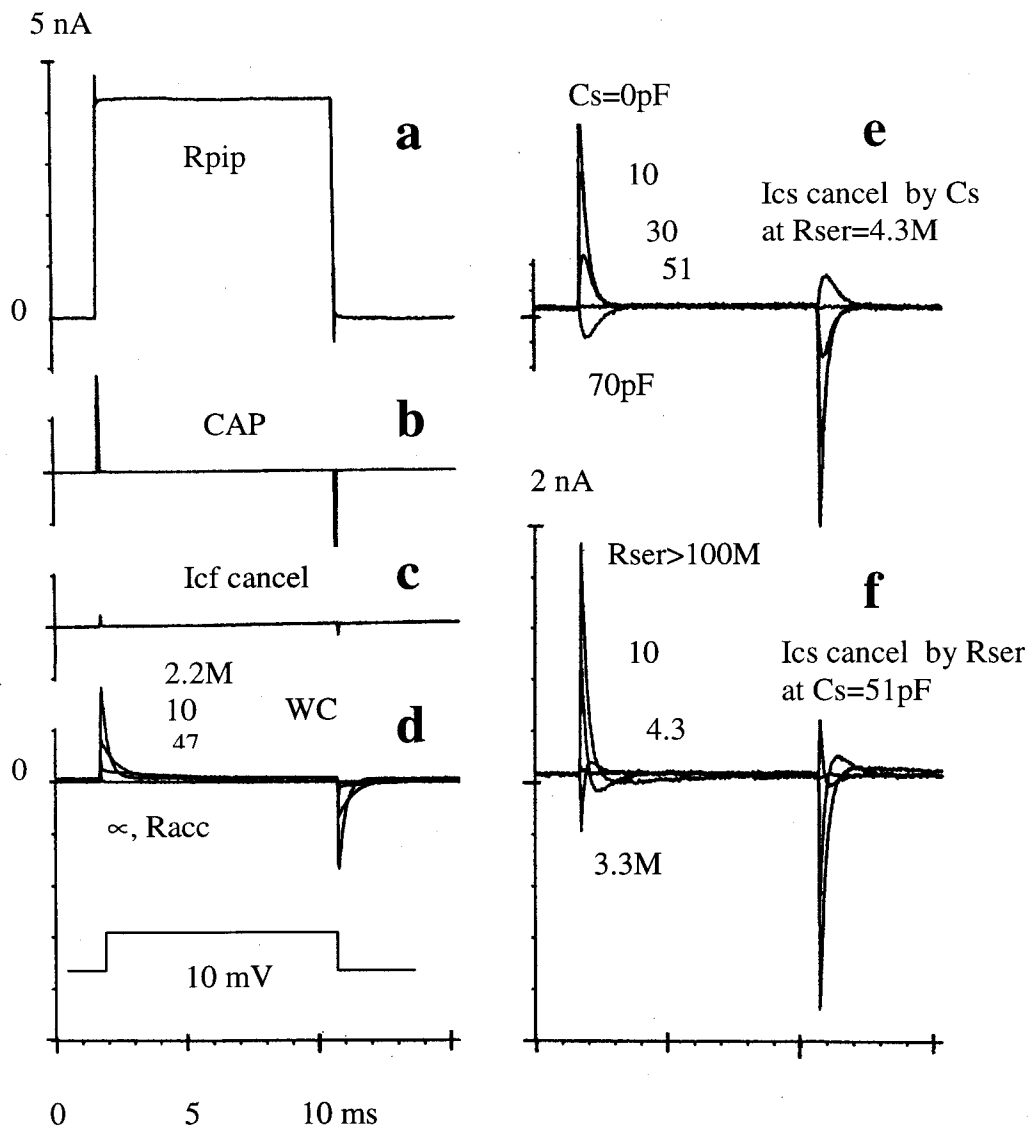


Figure 3.4. Experimental procedures for preparing a conventional whole-cell experiment, including fast capacity current (I_{cf}) and slow capacity current (I_{cs}) cancellation during 10mV voltage step application. Record a serves to calculate R_{pip} (here 2.2M), record b shows I_{cf} after giga-sealing, thus in the cell-attached-patch (CAP) configuration. Record c shows I_{cf} after almost complete cancelling. The records in frame d show the sudden appearance of I_{cs} upon establishing a WC from the CAP. The better the access to the WC (the lower R_{acc}), the higher and faster I_{cs} (examples $R_{acc} = \infty, 47, 10$ and 2.2M). Frames e and f illustrate the changes in I_{cs} during I_{cs} cancellation, in frame e for C_s adjustments (0-70pF) at the right R_{ser} value (4.3M) and in frame f for R_{ser} adjustments (>100M-3.3M) at the right C_s value (51pF). Low-pass frequency filter setting is at 10KHz. Other general conditions are as in Fig. 3.3.

Current-clamping the un-clogged pipette will not give the current-offset problem seen above for the open input. The tiny offset current may flow, but would only build up a tiny voltage on $C_{pc} + C_{pip}$, until the current through R_{pip} equals the offset current. That will be at a potential equal to $I_{offset} \times R_{pip}$, as explained at ERC-circuit 2. If $I_{offset} \sim 1pA$, then C_{pip} will be charged to $2\mu V$ ($1pA \times 2M\Omega$), which is small enough to be neglected. A $10G\Omega$ resistance would, however, be

polarized by 10 mV and an open input would change its potential by 1 Volt in 1 s (rate of change 1V/s, see equation 2.3). Thus, offset currents are particularly disturbing when measuring voltages from high resistance voltage sources.

The general **conclusions** from these experiments are:

- * Pipette capacity can simply be measured by cancellation when a pipette is clogged (non-conducting) in the outer tip.
- * Fast capacitance pipette currents overshooting steady pipette currents upon step stimulation of a (non-clogged) patch pipette can only be seen at minimal signal filtering. Thus, ERC-circuit 2 applies during R_{pip} and C_{pip} measurements.
- * The input resistance R_{vc} of the amplifier is small enough to carry out good measurements of $R_{pip} > 1M$.
- * Stray capacity of the pipette-holder and pipette capacity should be minimized when patch-clamp measurements require high frequency resolution. This can be done by using short leads, small size pipette holders and short patch pipettes with thickened glass tips (covered with Sylgard, a silicone coating), containing little filling solution and not deeply immersed in the bathing solution.

3.3.4. Giga-seals and canceling the fast capacity currents in the cell-attached-patch (CAP) configuration

Once the experimenter knows that his equipment functions properly and that his patch pipette has the right resistance (usually 1-3M Ω), i.e. not clogged or broken, he checks the pipette for offset potential in zero current-clamp or for offset current in zero voltage-clamp. He does this in order to compensate this offset with the use of the V_{pip} offset potentiometer on the patch-clamp. This will not be necessary for our model pipette, since it does not include a voltage source. The present model, however, provides the opportunity to check whether the zero voltage settings (V_{hold} and V_{pip} offset) of the amplifier are all right and whether there are other hidden voltage sources in the instruments to be compensated.

After the necessary checks and adjustments a cell is selected for a seal attempt. The pipette is gently pushed against the cell and slight suction is applied to initiate giga-sealing. Sealing may occur slowly (minutes) or very quickly (seconds). The obtained measurement configuration is the **cell-attached patch (CAP)**, so widely used for single-channel current recording. In practice, the appearance of spontaneous single channel activity is often the best proof of the establishment of a CAP.

In the present cell model sealing occurs abruptly, when switch S_{seal} (switch 5 in Fig. 3.1) is opened. This action represents the exchange of the short-circuit connection of the pipette to ground for the giga-seal resistance R_{seal} (20G Ω). It is illustrated in Fig. 3.3d-e (for <80KHz low pass (or >80KHz high cut-off) filtered records), where the open pipette response before sealing is indicated in panel d and the remaining fast capacitor current on- and off-spikes after sealing in panel e. These **giga-seal spikes** are practically the same as the spikes measured for the clogged pipette. In fact, after giga-sealing the pipette is clogged again, but now by a CAP with a very small capacitance C_{cap} and a very high resistance $R_{cap} = R_{mcap} = 20G$, shunted by $R_{seal} = 20G$. Thus, the apparent seal resistance $R_{capseal} = 10G$ (measurable at higher gains and voltage steps), since the **series resistance of the**

attached cell with $R_m < 1G$ may be (practically) neglected. The **membrane capacity C_m of the attached cell** may also be neglected, since the two capacities in series (C_{cap} and C_m) are equivalent to a capacitance

$$C_{capm} = C_{cap} \cdot C_m / (C_{cap} + C_m) \sim C_{cap}, \text{ for } C_m \gg C_{cap}.$$

Thus, for resistance and capacitance measurements on the CAP, it is as if the CAP is directly coupled to ground at its intracellular side. This is further illustrated below under 3.3.7 and in Fig. 3.6.

The **membrane potential of the attached** cell may not, however, be neglected. It is imposing its voltage on the CAP through the voltage-clamp circuit (as it would also do without the voltage-clamp!) and the voltage-clamp may add its voltage to that membrane potential. That is all what the voltage-clamp can do, change the existing membrane potential across the CAP. In certain applications it is a disadvantage that V_m is unknown or is not constant.

At zero voltage-clamp and in the absence of voltage sources in the CAP, V_m is the driving force for current through the CAP, sending current through the CAP and into the voltage-clamp, because the currents will not choose the high resistance path to ground through R_{seal} . This current, if significant, is seen in the voltage-clamp as a **small holding current**.

Under favorable conditions (high R_{seal} , no intrinsic E_{cap}) we can see part of V_m in zero **current-clamp recordings from a CAP**. In our model we expect to measure about $0.5V_m$, since V_m is voltage-divided over $R_{cap}(=R_{mcap})$ and R_{seal} . This can be confirmed after minimizing I_{offset} from the amplifier first, which is now very important because of the high resistance of the CAP and the seal.

We return now to the capacitance measurements (by I_{cf} canceling) to check whether the charging capacity in the fast capacity current transients is still $C_{pc} + C_{piphold} + C_{pip}$, as in the current transients charging the clogged pipette in the bath. This turns out to be roughly the case when using fast transient cancellation alone, as before. However, the canceling is not perfect and the values are not exactly the same. It looks as if one has to force fast transient cancellation with compromised C_f and τ_f settings. It is as if sealing has added a small and slower capacitance transient to the step response. The reason for this could be that connection of R_{pip} to the circuit adds R_{pip} as an extra series resistance to the stray capacitance (e.g. C_{cap}) of the circuit.

Fast capacity current cancellation is useful for C_{pip} measurement, but another use of this option is not less important: the **removal of the large sharp current spikes** from the voltage step responses. This is of particular importance for the responses to the larger voltage steps, as they can saturate the amplifier and spoil its high frequency performance. Clipping of signals because of amplifier saturation can be evoked by increasing the voltage step size under the conditions of the experiment of Fig. 3.3.

3.3.5. Whole-cell (WC) recording: measuring series resistance and cell capacitance while canceling the slow capacity transients

In many cases the CAP is only a transient stage toward reaching the final goal, the **whole-cell (WC)** configuration. As explained in Chapter 1.2, WC-conditions are obtained by breaking the CAP while maintaining the giga-seal to the attached cell. If this is done during voltage-clamp stimulation with voltage steps, one can easily conclude from the responses whether a WC is obtained and whether the quality of the WC is good enough to proceed with the planned experiment. This procedure will be demonstrated now.

With the model cell (Figs. 3.1 & 3.2) one can simulate WC-formation by closing switch Sacc (#7). This action causes shunting of Rmcap by Racc, as illustrated by the experiment of record f in Fig. 3.3, where Racc=2.2MΩ. Record f shows that WC-formation causes the sudden appearance of an extra, slow capacitor current transient upon voltage-step stimulation. This slow transient is much smaller in amplitude (~2nA) than the fast capacitor transient (~12nA, at 80KHz filtering) and its time constant τs (~0.25ms) >> τf (~2.5μs). The observed amplitude and time constant are consistent with the slow component properties of ERC-circuit IV (Fig. 2.4), with Rp=4.4MΩ (the series resistance Rser = Rpip + Racc) and Cm = 50pF in the present case.

The predicted amplitude is $10\text{mV}/4.4\text{M}\Omega = 2.2\text{nA}$ and the predicted $\tau_s = 4.4\text{M}\times 50\text{pF} = 0.22\text{ms}$. The steady-state change in current of $10\text{mV}/1\text{G}\Omega = 10\text{pA}$ cannot be seen on the current scale of Fig.3.3.

The experienced patch-clamper routinely estimates Rser = Rpip + Racc from the peak height of the slow capacitance transient on the oscilloscope or PC screen and Cs = Cm from the time constant τs. She will then know whether Rser is low enough to continue the experiment on the whole-cell (WC) obtained, or try to get better access to the WC (lower Racc) by extra suction. In the newer Windows versions of the Axon Instruments patch-clamp acquisition software (pClamp7 and 8 and 9) Rser, Cs and τs are calculated on-line from the records. When Rser is satisfactory, the experimenter starts to cancel the slow capacitor transient in order to obtain flat control records for easier recognition of voltage-activated currents evoked by larger voltage steps.

The **canceling procedure** is illustrated in Fig. 3.4 for the same electronic cell as in Fig. 3.3, but at an increased current resolution, which is closer to regular experimental practice. High frequency cut-off filtering is now at 10KHz. The current through the pipette in the bath is as expected for a 2.2MΩ pipette resistance (frame a). After giga-sealing the fast capacity current transient (Icf) remains (frame b). This transient must be cancelled (frame c) to prevent amplifier saturation at higher current gains and voltage steps and to better be able to recognize the shape of the slow capacitance current transient (Ics) of the whole-cell. WC-transients Ics are illustrated in frame d, where the curve labeled Racc = 47MΩ exemplifies a "bad" WC, in which CAP perforation is incomplete so that Racc remains high ("small CAP hole"). Ics improves if Racc = 10MΩ is taken, but it is best (high and fast) if Racc = 2.2MΩ. Remember that it is Rser that matters for the shape of Ics, and that Rser = Rpip + Racc = 2.2MΩ + Racc. The lower Rser, the higher and the faster is Ics, thus the sooner the cell membrane is charged to the clamped potential (10mV here). In practice, similar successive Ics transients as in Fig. 3.4d may be obtained during successive attempts (repeated suction pulses) to get better and better WC-conditions on the same cell. They may occur in reverse order if WC-conditions deteriorate due to closure of the hole in the CAP-membrane (resealing of the ruptured CAP-membrane). Rser = 2Rpip is usually considered the best obtainable WC-condition.

Notice also that breaking into the cell causes a small holding current because of the appearance of the membrane potential ($= E_l = \sim -60\text{mV}$, measurable in current-clamp after careful zeroing input offset current) and conductance ($= G_l = 1/R_l$) in the circuit. This would produce $\sim 60\text{mV} / 1\text{G} = 60\text{pA}$ outward (positive) current at the holding potential of 0mV . The 10mV voltage step would add another 10pA , but the resolution in Fig.3.4 is too low to precisely measure these current changes.

Frames e and f show how the records look like during the **Ics cancellation** procedure. In frame e C_s is increased from 0 to 70pF at exactly the right $R_s = 4.3\text{M}\Omega$ value, close to the expected value of $R_{\text{pip}} + R_{\text{acc}} = 4.4\text{M}\Omega$ (nominal value). At 51pF the response is exactly flat, at smaller C_s the response is positive, while the responses are negative at too large C_s values (e.g. 70pF). But all transients are mono-phasic, whether they are positive or negative.

In frame f, R_{ser} is adjusted at exactly the right C_s . R_{ser} is decreased from $>100\text{M}\Omega$ to 10 , 4.3 and $3.3\text{M}\Omega$. At $4.3\text{M}\Omega$ cancellation is perfect (flat record). Both at higher and lower R_{ser} the current transients are biphasic. At higher R_{ser} ($10\text{M}\Omega$), the biphasic transient is positive-negative. At lower R_{ser} ($3.3\text{M}\Omega$) I_{cs} is negative-positive. From these examples one may derive a quick procedure for I_{cs} cancellation for obtaining flat current records despite the abrupt steps in voltage. Quick action is required, since cancellation time is at the expense of experiment time.

First, quickly adjust C_s to a value estimated in the physiological range. Second, dial R_s to a value at which there is neither an initial overshoot nor an initial undershoot. Third, adjust C_s to flat or almost flat records. In the latter case R_{ser} and C_s may need fine-tuning according to the same procedure.

The **biphasic nature of the records** in frame f can easily be understood from the nature of the cancellation procedure. I_{cs} has, under ideal conditions, a single exponential shape, in which the peak current is equal to $\Delta V/R_{\text{ser}}$ and the time constant of the decay is equal to $R_{\text{ser}}C_m$. When the cancellation procedure is carried out, the amplifier produces from the voltage step an exponential current transient of opposite polarity to I_{cs} at the input of the amplifier. The peak of this opposite transient is determined by the value on the dial that cancels R_{ser} , while the dial that cancels C_s determines the time constant of the decay of the cancelled transient according to $R_{\text{ser}}C_s$. If the canceling R_{ser} is smaller than the real R_{ser} but at approximately the right canceling C_s , the canceled transient is larger in peak size and shorter in duration than the real I_{cs} . Thus, the addition of the negative canceling transient to the positive real transient results in an initial negative peak. Furthermore, because of the shorter canceling transient, canceling occurs only in the first part of I_{cs} , thus the second part of I_{cs} is not cancelled and remains positive. In this way the negative-positive I_{cs} transient arises at $R_{\text{ser}} = 3.3\text{M}\Omega$ in Fig. 3.4f. In a similar way the positive-negative capacity transients at canceled R_{ser} values that are too large can be explained. Insight in the origin of the shape of the partially cancelled transients helps in following a quick and rational procedure for capacity transient cancellation. This also applies to I_{cf} canceling, though the condition may look a bit more difficult, because the extremely fast I_{cf} transients (μs time constants) are usually distorted even by the best amplifier filter settings. Reconstruction of the various incompletely cancelled I_{cs} shapes is best illustrated by drawing by hand the summation of various I_{cs} transients and various canceling exponential transients of opposite polarity.

The R_{ser} value read from the canceling dial is an important indicator of the quality of voltage-clamp conditions (the lower R_{ser} , the better, see Chapter 2), while the $C_s = C_m$ value that is determined is important for normalizing the current records to cell size (reflected in C_m). Since R_{ser} may change during an experiment, R_{ser} should be checked by I_{cs} cancellation regularly in the course of an experiment. **The first indication of R_{ser} changes after perfect I_{cs} canceling is the appearance of biphasic I_{cs} transients** in the records, positive/negative if R_{ser} improves (i.e., decreases) and negative/positive if R_{ser} increases, as can be understood now from the above explanations.

It is important to emphasize here that I_{cs} cancellation is only a safety against amplifier saturation and a cosmetic procedure, because it does not improve the voltage-clamp conditions. The flat base line may give better records for current recognition. However, if you would record the membrane potential with an independent electrode during a voltage-clamp step after I_{cs} cancellation, you would observe that the membrane potential still follows the applied voltage step with an exponential transient with time constant $R_{ser}C_m$ (see the model experiment of Fig. 3.9). As a rule, only after $\sim 3X$ the time constant is the membrane potential actually clamped to the applied potential. For this reason, experimenters may sometimes choose not to fully cancel I_{cs} , keeping a small I_{cs} visible to remind themselves of the actual duration of the membrane potential transient in the cell. Thus, it remains important to make R_{ser} as small as possible.

3.3.6. Pulling an outside-out patch (OOP) and checking the seal resistance

As explained in Chapter 1.2, the **outside-out patch (OOP)** is obtained by gently pulling a vesicle from the WC. Thus, the OOP is a micro-WC with only one or a few channels. An exception is when a large vesicle is drawn or channel density is very high in the OOP. The OOP allows the patch-clamper to study single-channel activation kinetics and co-operative channel behavior. With the present equivalent-circuit cell model we demonstrate a few OOP properties of methodological interest.

Fig. 3.5 shows how the slow capacity current (I_{cs}) changes upon establishing the OOP measurement configuration. I_{cwc} in frame a shows a non-cancelled I_{cs} in the WC configuration (I_{cf} is cancelled!). It is from the same electronic cell as in Fig. 3.4. After perfect I_{cwc} transient cancellation at $R_{ser} = 4.3M\Omega$ and $C_s=51pF$, the record is flat (see arrow). Pulling a successful OOP by opening switch S_{oop} (switch 9 in Fig. 3.1) suddenly causes the **appearance of a large inverted exponential transient** of a similar size as that of I_{cwc} . An OOP attempt is unsuccessful if the seal is lost during pulling up of the pipette. In that case, the 10mV voltage step causes a very large off-screen current response and the holding current may already jump off-screen at small offsets or holding potentials. This does not happen here, because $R_{seal}=20G\Omega$ is kept constant. Here, we observe a small change in holding current, since the membrane potential ($E_l \sim -60mV$) is no longer in series with $R_l = 1G\Omega$, but with the much larger $R_{oop} = 20G\Omega$.

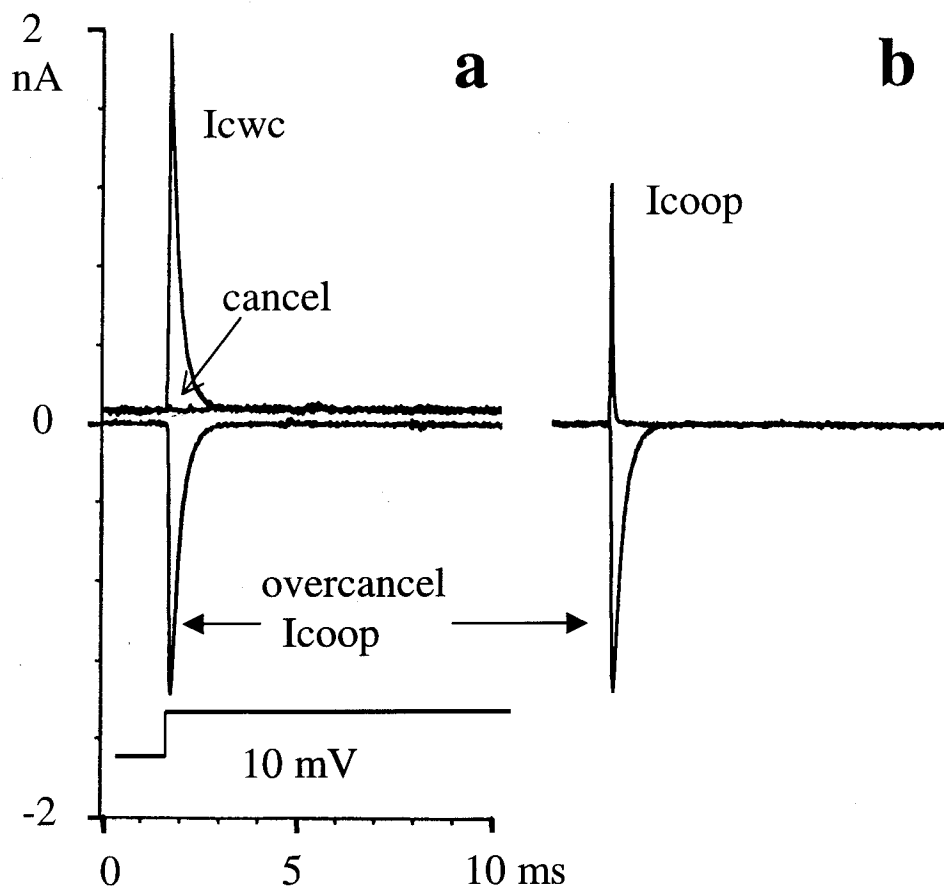


Figure 3.5. Slow capacity current (I_{cs}) changes upon establishment of the outside-out-patch (OOP) measurement configuration. The model cell and the test pulse are the same as those in Fig. 3.4. I_{cwc} is the uncanceled I_{cs} of the WC (frame **a**) and I_{coop} is the uncanceled I_{cs} of the OOP (frame **b**). The flat record in frame **a** is the perfectly cancelled I_{cwc} , while the negative records in frames **a** and **b**, labeled overcancel(ed) I_{coop} , are the records obtained just after OOP formation from the condition of perfect I_{cwc} cancellation (flat record in frame **a**). The sudden appearance of the large inverse I_{cwc} -like current transient is indicative for the formation of an OOP. Notice that $E_l = E_{oop} \sim 60\text{mV}$ in this experiment, as in Figs. 3.3 and 3.4.

The inverted transient is, in fact, an overcompensated I_{coop} response revealing the major part of the I_{cwc} canceling transient causing the flat record in frame **a**. This over cancelled I_{coop} is not exactly equal to an inverted I_{cwc} , because there is a remaining I_{coop} made visible in frame **b** by removing transient cancellation with the switch on the amplifier. Without I_{cs} cancellation one would see a change from I_{cwc} (Fig. 3.5, frame **a**) to I_{coop} (frame **b**) upon OOP-formation. I_{coop} could be perfectly cancelled at the same series resistance $R_{ser} = 4.3\text{M}\Omega$ as for canceling I_{cwc} , but with a much smaller capacitance $C_s = 6.1\text{pF}$. Although this C_s value is larger than the nominal value of $C_{oop} = 3.3\text{pF}$, it is quite acceptable, because the nominal value is imprecise and the circuit easily adds a few pF stray capacitance to this nominal value. The important observation is that R_{ser} has the same value as that for I_{cwc} cancellation. This implies that I_{cwc} and I_{coop} should have the same peak current (see theory of ERC-circuits I-IV). Frame **b** shows that I_{coop} has a smaller peak than I_{cwc} . This is due to the use of the 10KHz-filter, which affects the very short I_{coop} more than the larger duration I_{cwc} . Changing the filter to 80KHz indeed increased the I_{coop} peak to that of I_{cwc} .

A few current-clamp observations are instructive. After careful zeroing current offset with the CCzero screw, V_m of the WC (V_{mwc}) was measured to be -57.8mV . For V_{moop} one would expect approximately $V_{mwc}/2$, because of **voltage division of $E_I \sim -57.8\text{mV}$ over R_{oop} (20Gohm) and R_{seal} (20Gohm)**. V_{moop} was found to have the expected value of -28.9mV .

The general **conclusion** from these observations is that one easily recognizes the formation of a good OOP from an I_{cs} -cancelled WC by the sudden appearance of an inverted I_{cwc} and the maintenance of high resistance conditions (R_{seal} not affected). Pulling an OOP can sometimes even serve as a test to see whether a high apparent WC conductance is due to a high membrane conductance or to a bad seal (low R_{seal}). In current clamp of the OOP, voltage division of the membrane potential over the various resistors of the circuit was as expected, provided the input offset-current was well zeroed.

3.3.7. Excision of an inside-out patch (IOP)

An inside-out patch (IOP) is obtained by excision of a CAP from the attached cell by a sudden pull-up of the sealed patch pipette. In the above discussion of the CAP configuration we argued that the RC-properties of the CAP and the attached cell membrane hardly contribute to the response of a giga-sealed CAP to voltage-step test pulses. The measured spikes (Fig. 3.3e), though heavily filtered, were mainly reflecting C_{pip} charging through R_{vc} . Thus, one would expect that these **spiky test responses of a CAP would not change upon excision of an IOP**. This turns out to be the case in the model cell experiment of Fig. 3.6, where the IOP was obtained by switching S_{iop} (switch 8 in Fig. 3.1) to ground connection from the CAP. Frame a shows a non-cancelled fast capacity current (I_{cf}) response of a CAP to stimulation with 10-mV voltage steps, while amplifier setting was at 10 kHz (low pass). The record shows perfect giga-sealing. In frame b the CAP- I_{cf} was largely cancelled. Frame c shows the I_{cf} record after IOP excision. It is practically the same as the CAP record in frame b. Therefore, this record shows maintenance of giga-seal conditions rather than any electrophysiological change, which is in contrast to the capacity current changes upon OOP formation from the WC (Fig. 3.5). Apparently, the large cell membrane capacity ($\sim 50\text{pF}$) does not contribute to I_{cf} , because it cannot be accessed for charging by E_{vc} through R_{vc} . It is only accessible through $R_{pip} + R_{cap}$, which is here very much larger ($\sim 20\text{G}\Omega$) than R_{vc} ($< 100\text{K}$). We would rather expect a tiny, but slower capacity current component for charging C_{cap} (a few pF) through R_{pip} ($2.2\text{M}\Omega$), unaffected by IOP excision because of the large differences between the access resistances R_{pip} (for C_{cap}) and $R_{pip} + R_{cap}$ (for C_m). This tiny component is not resolved in the records of Fig. 3.6.

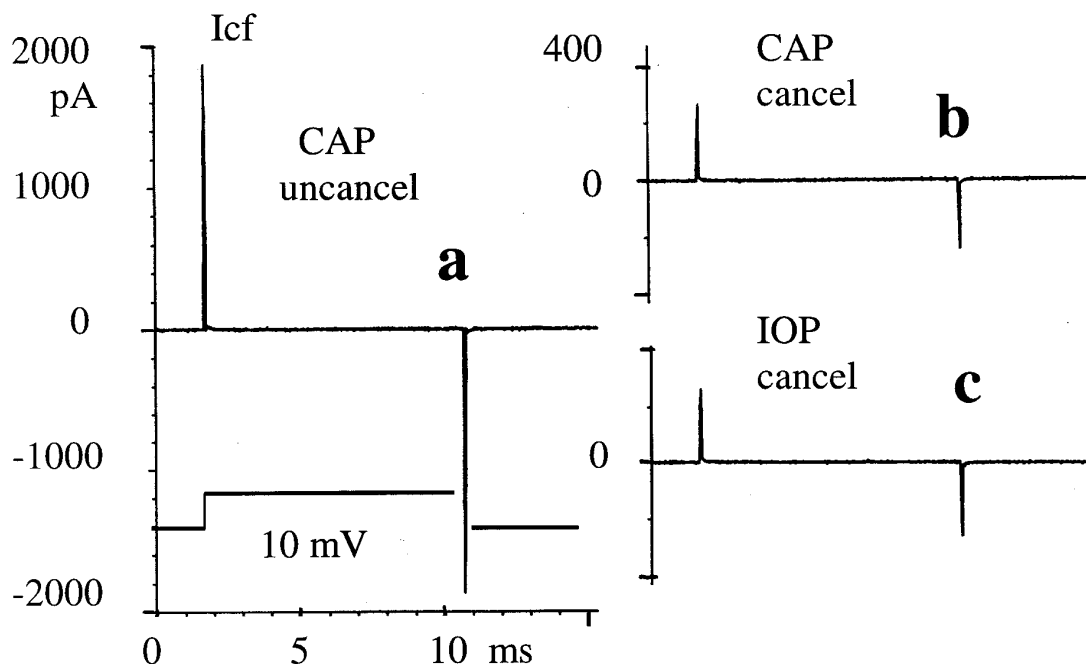


Figure 3.6. Fast capacitive current (I_{cf}) transients of the cell-attached-patch (CAP) and inside-out-patch (IOP) compared. The uncanceled CAP- I_{cf} transients in frame a are the same as those in Fig. 3.4b for the same experimental conditions. Largely cancelled CAP- I_{cf} transients are shown in frame b. Essentially the same I_{cf} transients are seen in frame c after excision of the CAP to obtain an IOP (by switching S_{iop} , switch 7 in Fig.3.1, to ground connection). I_{cf} was largely rather than fully cancelled in frames b and c, in order to be able to better observe changes in I_{cf} upon uncoupling the cell from the CAP.

However, the **disconnection of the membrane potential** of $V_m = -60\text{mV}$ from the CAP must have some consequence. It drives a holding current of $-60\text{mV}/20\text{G}\Omega = -3\text{pA}$ through the CAP and it is this current, which must have disappeared in the IOP. The resolution in the records of Fig.3.6 is too low to observe this change. During high-resolution recording of CAP-channel activity under favorable conditions, one may be able to see such changes. However, **changed channel activity** will probably be a more significant indication of the change from CAP to IOP. This is because the loss of the membrane potential will alter voltage dependent channel activity and the loss of the intracellular chemical environment will cause the disappearance of intracellular ion channel activators or inhibitors (Weidema et al., 1993).

3.3.8. Making a permeabilized-patch WC (ppWC)

The formation of ppWC conditions during nystatin or amphotericin (channel forming antibiotics) incorporation in the CAP can elegantly be followed from the **gradual development of an increasing slow capacitor current (I_{cs})**. This process has already been demonstrated in Fig. 3.4d, where WC conditions improved in steps from $R_{acc} = 47\Omega$ to $R_{acc} = 2.2\text{M}\Omega$ by applying “successive suction pulses.” The three increasing I_{cs} transients may also be seen as three examples from a gradually growing I_{cs} during ppWC development. The increase in the I_{cs} peak would reflect the decrease in R_{acc} due to permeabilization of the CAP by the antibiotic. The immediate consequence of a decreasing R_{ser} is a decrease of the decay time constant ($R_{ser}\cdot C_m$) of I_{cs} . Thus,

the better the permeabilization, the faster and closer the WC membrane is charged to the applied potential.

Current-clamp potential measurements are again instructive. Long before CAP permeabilization is satisfactory for reliable voltage-clamp recording, conditions may be favorable for zero current-clamp membrane potential measurements if the recording pipette is filled with an intracellular-like solution. For example, at $R_{ser} \sim R_{acc} = 100\text{M}\Omega$ (bad ppWC), V_{mwc} measurements are already acceptable within 10% for R_{seal} values $>1\text{G}\Omega$, provided input offset-current is well cancelled. In Fig. 3.4d, $V_{mwc} = -58\text{mV}$ at $R_{acc} = 47\text{M}\Omega$, which is practically equal to the $V_{mwc} = -59\text{mV}$ at $R_{acc} = 2.2\text{M}\Omega$ (at $R_{ser} = 4.4\text{M}\Omega$, a very good ppWC).

3.4. An instructive model experiment

We describe below one whole-cell model experiment, which is very relevant for daily patch-clamping. Several more instructive model experiments are suggested in PlenumBTOL.

Checking whole-cell membrane potential and resistance

One of the first actions of an experimenter after obtaining the WC patch-clamp configuration is measuring the resting V_m and R_m in the current-clamp mode. A sufficiently negative V_m and high R_m is often a criterion for accepting a cell as a good cell for a continued experiment. Therefore, we demonstrate these measurements here on our model cell (Fig. 3.1) and show how the conductance properties of a cell determine the membrane potential and resistance properties and, in combination with membrane capacity, also the time constant of the V_m response of the membrane to current pulses. We apply here the theory explained in Chapter 2.3 and 2.4 (parallel conductance equations and exponential transients on current stimulation).

Fig. 3.7 shows observations from such an experiment for experimental conditions further described in the legend of the figure. In Fig. 3.7a V_m was recorded as a function of time while successively inserting and removing conductance branches with the switches 11 and 12 in Fig. 3.1. In Fig. 3.7b $V_m(t)$ was recorded upon stimulation by current blocks of 100pA for the cell membrane in 3 different conductance states.

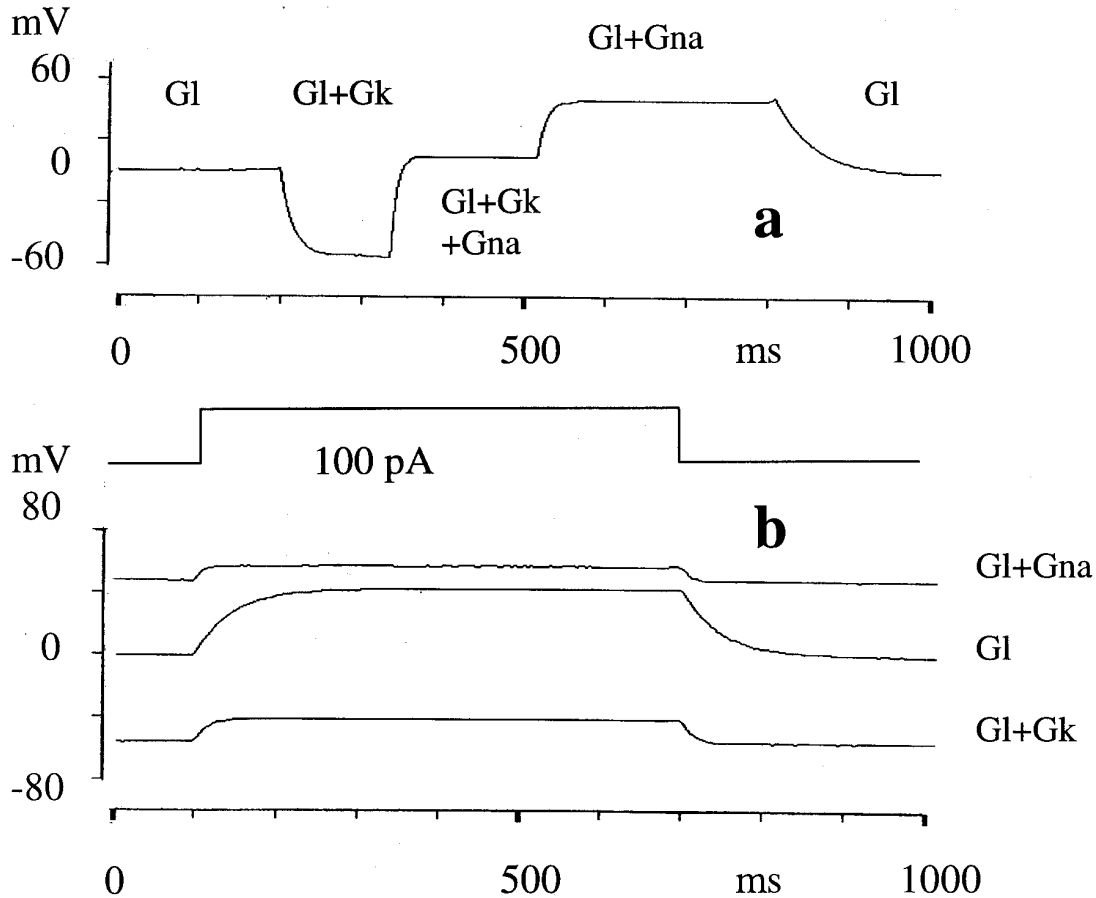


Figure 3.7. Whole-Cell membrane potential changes upon sudden conductance changes (a) and upon current-step stimulation (b) Gk and Gna were switched on and off with the use of a reed contact in series with Gk and Gna, which can be operated by approaching it with a small magnet. In the initial condition of the experiment of figure a only the Gl branch of the 3 conductance branches Gl, Gk and Gna was switched on (Sgl on and Sgk and Sgna off, see Fig. 3.1), which caused the initial $V_m = E_l = 0\text{mV}$. At $\sim 200\text{ms}$ Sgk was also switched on, which resulted in a hyperpolarization towards $E_k = -86\text{mV}$. At $\sim 340\text{ms}$ Gna was added, causing a depolarization towards $E_{na} = +60\text{mV}$. At $\sim 500\text{ms}$ Gk was switched off, causing a further depolarization towards E_{na} . When finally Gna was switched off at $\sim 800\text{ms}$, V_m returned to the initial $V_m = E_l = 0\text{mV}$. In figure b the cell was stimulated by a 100pA block-pulse current in the 3 conductance states of figure a indicated. The responses reflect the RC-properties of the membrane in the 3 conductance states. Other circuit model properties: $R_{\text{pip}} = R_{\text{acc}} = 2\text{M}$, $R_l = 400\text{M}$, $R_k = 200\text{M}$, $R_{na} = 100\text{M}$, $R_{\text{seal}} = 20\text{G}$, $R_{\text{cap}} = 20\text{G}$, $C_m \sim 86\text{pF}$ and $C_{\text{pip}} \sim 5\text{pF}$ (measured by cancellation).

The initial membrane potential was $V_m = 0\text{mV}$, since initially Gl with $E_l = 0\text{mV}$ was the only conductance present in the membrane. Upon activating Gk, V_m hyperpolarizes towards $E_k = -86\text{mV}$. The observed $V_m = -56.2\text{mV}$, which is E_k divided over R_k and R_l , is close to the value $V_{lk} = -57\text{mV}$ calculated from the general equation for the membrane potential V_{m12} of a cell with two parallel membrane conductances

$$V_{m12} = (G_1 E_1 + G_2 E_2) / (G_1 + G_2).$$

This equation has already been used above in another context in its resistance form (cf. Eq. 23). In that context one of the two parallel conductance branches was that of the cell (with E and R), while

the other was that of the voltage-clamp voltage source E_s in series with the voltage-clamp source resistance R_s). Eq. 37 is another example of this two-conductance (resistance) parallel equation. Upon additional activation of G_{na} , V_m becomes +9.6mV, close to the calculated value $V_{lkn} = +9.4\text{mV}$, calculated from a general equation for the membrane potential V_m of a three-parallel conductance membrane

$$V_m = (G_1 E_1 + G_2 E_2 + G_3 E_3) / (G_1 + G_2 + G_3).$$

Deactivation of G_k results in $V_m = +47.2 \text{ mV}$, close to the calculated $V_{ln} = +48\text{mV}$ (see the above equation for V_m).

The transients between the conductance states are single-exponential with time constant values to be calculated from the inverse values of the sum of the active conductances (equivalent values of the active resistances) times the membrane capacitance (cf. Eqs. 14 &15 and 24 & 25). The higher the conductance, the faster the time constant. The slowest time constant occurs when the membrane is in the G_l state and is $RI C_m = 400\text{M } \Omega \times 86 \text{ pF} = 344 \text{ ms}$ (cf. last part of record in Fig. 3.7a).

The V_m responses to the current steps (panel b) are consistent with these observations. The higher the membrane resistance, the larger and the slower the V_m -responses. The time constants of the current responses in the various G -states in panel b are equal to those in the V_m transients to those states in panel a.

G_l is not the dominant conductance and V_m is not too depolarized, thus such a cell would in reality probably be acceptable for the study of G_k or G_{na} , though a smaller G_l would be better. One cannot conclude from the records in Fig. 3.7 whether G_l is a membrane conductance or a leaky seal. The behavior of the circuit in figure a can serve as a model for effects of opening and closing of single ion channels on V_m of a cell with only a few channels, but also for effects of abrupt activation of a conductance consisting of a large collection of channels. Usually, activation of a conductance involves successive activation of channels with certain kinetics, but it is good to realize that even in that case sufficient time resolution of such records should, in principle, reveal effects of each channel opening on V_m as illustrated in Fig. 3.7 for a cell with only 3 (big!) channels.

3.5. Conclusion

After the practical exercises of the present chapter on the electrical equivalent circuit model, you may have experienced that it is not always easy to **recognize the simple theoretical concepts** of the previous chapter in the measurement configuration and the model cell properties. In a real patch-clamp experiment this is even more complex. First, the cell is much more complex, i.e. has many more “hardware” components (ion channel types, ion pumps and exchangers). Second, one cannot see and easily remove or substitute these components. Third, the cell components are usually unknown. Finally, the electrical properties of a cell are often changed during an experiment. Therefore, the experience gained in the present exercises will help to recognize cell properties from artifacts and the new and unusual electrical properties of a cell from its standard properties.

One complication seen in the simulation experiments was the **deformation of the fast capacity current transient by the amplifier**. The filter inside the amplifier reduced the peak and increased the duration of the transient compared to estimated peak and time-constant values for a simple

ERC-circuit of the voltage-clamp condition. To understand this we need to add an extra capacitance, C_{vc} (Fig. 3.1), to the simple ERC-circuits of voltage-clamp stimulation explained in Chapter 2. This is further explained in PlenumBTOL.

The effects of **stray capacitance** were striking. The way they affected the fast capacitor transient (peak increase) could also be understood from an ERC-circuit including C_{vc} . These observations indicated the importance of minimizing stray capacitance when trying to obtain the best possible time resolution for studying ultra-fast conductance changes upon voltage steps.

The **establishment of the various patch-clamp configurations** could be recognized from electrical changes during the manipulations, except for the IOP. CAP-formation was easily followed from the disappearance of the pipette current during giga-sealing. WC- and ppWC-formation are evident from the sudden and the gradual appearance, respectively, of the slow capacitor current transient. OOP-formation has occurred when the slow capacitor transient suddenly shortens or when a cancelled transient suddenly becomes strongly over-cancelled. IOP-formation cannot be concluded from simple electrical changes, but is signaled by electrophysiological changes, e.g. the disappearance or change of CAP-channel activity or the appearance of new channel activity. The four other configurations are also to be confirmed by electrophysiological changes, e.g. the appearance of typical WC-currents upon voltage stimulation. Analysis of slow capacity transient cancellation resulted in a prescription for a simple and quick cancellation procedure.

The **current-clamp measurements in the CAP and the WC** were instructive, since they showed how important it is to minimize amplifier offset current effects for reliable potential measurements from high-resistance sources. Of special and practical interest were the measurements of the membrane potential, V_m , of a cell through a cell-attached patch or of fractions of V_m depending on voltage division over R_{cap} and R_{seal} . The WC-current clamp experiments illustrated the standard properties of a membrane with linear ion conductances, consistent with the parallel conductance equation. Simple, single exponential RC-response behavior was seen upon current step stimulation.

We did not touch all practical procedures and problems of importance for patch-clampers. For example, **series resistance compensation** was not discussed, though most patch-clamp amplifiers have this compensation as an option. However, we have seen the importance of minimizing R_{ser} to improve voltage-clamp quality. One may, for example, use patch pipettes with larger tip diameters to get lower pipette resistances (and therefore lower R_{ser}). Nevertheless, minimized R_{ser} values may still be too large for large and fast currents such as Na currents. Engineers have therefore developed a technique to lower R_{ser} by electronic means inside the amplifier. This R_{ser} compensation procedure is not merely cosmetic (as it was for I_{cs} cancellation!), but it actually improves voltage-clamp as if R_{ser} has really been reduced. After this ERC-course you may now understand that this point can be verified by checking sharpening up of the I_{cs} transient!

A last problem to be mentioned is that intracellular voltage clamp may be poor for other reasons than a $R_{ser}C_m$ time constant that is too large. If the cell is not a simple sphere but has complex morphology (e.g. a neuron with axon and dendrites), or if it is coupled to other cells through gap junctions (Harks et al., 2003), then the voltage is only clamped in the membrane near the electrode and not more distally. This condition is called “lack of space clamp”. Electrophysiologically, poor

space clamp can be recognized from the non-single exponential shape of the slow capacity current transient (Torres et al., 2004).

Finally, we hope that we have provided the student with two valuable tools to do real patch-clamp experiments. The first is **thinking in terms of simple electrical equivalent circuits of cells**. The second is experimenting on cells as if they actually have these electrical equivalent circuits to help you answer your research questions.

Good luck with your experiments!

Table 3.1. Component abbreviations, used or recommended component values (nominal or estimated) in the model cell experiments and full names of the components The components are listed in groups and, within the groups, from left to right and clock-wise in the circuit. The abbreviations CAP, WC, OOP and IOP are explained in Fig. 1.1. In some experiments magnet operated reed contacts were used for the switches S6, S11 and S12.

COMPONENT	VALUE(S)	NAME
Rcc	>> 100G (amplif. specif.)	current-clamp Resistance
Rvc	<< 1 M (amplif. specif)	voltage-clamp Resistance
Rpip	2 or 2.2 M	pipette Resistance
Rseal	10 or 20 G	seal Resistance
Rcapch	1 or 2 G	CAP channel Resistance
Rmcap	10 or 20 G	CAP membrane Resistance
Racc	2, 2.2, 5, 10 M	access Resistance
Roop	10 or 20 G	OOP Resistance
Rl	400M, 1 G	leak Resistance
Rk	200 M	potassium Resistance
Rna	100 M	sodium Resistance
Rser	Rpip+Racc	series Resistance
Gl	1/Rl	leak Conductance
Gk	1/Rk	potassium Conductance
Gna	1/Rna	sodium Conductance
Cpc	~1 pF (see amplifier specs)	patch-clamp Capacitance
Cpiphold	~1 pF	pipette-holder Capacitance
Cpip	4.7 pF	pipette Capacitance
Ccap	~ 1 pF (stray cap. of circuit)	CAP Capacitance
Coop	3.3 pF	OOP Capacitance
Cm'	47 or 94 pF	membrane' Capacitance
Cm (=Cwc=Cm'+Coop)	~ 50 or ~100pF (excl. Ccap)	WC membrane Capacitance
Cvc	amplifier specs	Internal vc Capacitance
Epc		patch-clamp Voltage source
Evc	-100 to +100 mV	voltage-clamp Potential
Ecc		current-clamp Potential
Eoop	0 or ~-60 mV	OOP membrane Potential
El	0 or ~-60 mV	leak reversal Potential
Ek	-60 to -90 mV	potassium Nernst Potential
Ena	~ +60 mV	sodium Nernst Potential
Scvc (S1)		cc-to-vc Switch
Spc (S2)		patch-clamp Switch
Scpip (S3)		pipette capacitance Switch
Srpip (S4)		pipette resistance Switch
Sseal (S5)		seal Switch
Scapch (S6)		CAP channel Switch
Sacc (S7)		access resistance Switch
Siop (S8)		IOP Switch
Soop (S9)		OOP Switch
Sgl (S10)		Gl Switch
Sgk (S11)		Gk Switch
Sgna (S12)		Gna Switch

REFERENCES

- Buisman** HP, De Vos A, Ypey DL. A pipette holder for use in patch-clamp experiments. *J Neurosci Meth* 31, 89-91, 1990.
- Gaspar** R, Weidema AF, Krasznai Z, Nijweide PJ, Ypey DL. Tetrodotoxin-sensitive fast Na⁺ current in embryonic chicken osteoclasts. *Pfluegers Arch (Eur J Physiol)* 430, 596-598, 1995.
- Hamill** OP, Marty A, Neher E, Sakmann B, Sigworth FJ. Improved patch clamp techniques for high resolution current recording from cells and cell free membrane patches. *Pfluegers Arch. (Eur. J. Physiol.)* 391, 85-100, 1981. (Appendix in Sakmann and Neher, 1995).
- Harks** EGA, De Roos ADG, Peters PHJ, De Haan LH, Brouwer A, Ypey DL, Van Zoelen EJJ, Theuvenet APR. Fenamates: A novel class of reversible gap junction blockers. *J Pharmacol Exper Therapeut* 298, 1033-1041, 2001.
- Hille** B. *Ionic Channels of Excitable Membranes*. Sinauer Associates, Sunderland, MA, 2001.
- Hines** M, and Carnevale NT. The NEURON simulation environment. *Neural Computat* 9, 1179-1209, 1997.
- Hirsch** MW, Smale S. *Differential equations, dynamical systems, and linear algebra*. Academic Press, San Diego, New York, 1974.
- Horn** R, Marty A. Muscarinic activation of ionic currents measured by a new whole cell recording method. *J Gen Physiol.* 92, 145-159, 1988.
- Horowitz** P, Hill W. *The Art of Electronics*. Second edition. Cambridge University Press, Cambridge, UK, 1990.
- Ince** C, VanBavel E, VanDuijn B, Donkersloot K, Coremans A, Ypey DL, Verveen AA. Intracellular microelectrode measurements in small cells evaluated with the patch-clamp technique. *Biophys J* 50, 1203-1209, 1986.
- Kandel** ER, Schwartz JH, Jessell TM. *Essentials of Neural Science and Behavior*. International Edition, Prentice Hall International, London, 1995.
- Neher** E, Sakmann B. Single-channel current recorded from membrane of denervated frog muscle fibers. *Nature* 260, 799-802, 1976.
- Neher** E, Sakmann B. The patch-clamp technique. *Sci Am* 266, 28-33, 1992.
- Neher** E. Ion channels for communication between and within cells. *Science* 256, 498-502, 1992.
- Ravesloot** JH, Van Putten MJAM, Jalink K, Ypey DL. Analysis of decaying unitary currents in on-cell patches of cells with a high membrane resistance. *Am J Physiol* 266 (Cell Physiol 35), C853-C869, 1994.
- Sakmann** B. Elementary steps in synaptic transmission revealed by currents through single channels. *Science* 256, 503-512, 1992.
- Sakmann** B, Neher E. *Single-Channel Recording*. Plenum Press, New York and London, 1995.
- Sherman-Gold** R (editor). *The Axon Guide for Electrophysiology & Biophysics Laboratory Techniques*. Axon Instruments, Inc., Foster City, CA 94404, USA, 1993.
- Torres** JJ, Cornelisse LN, Harks EGA, Van Meerwijk WPM, Theuvenet APR, Ypey DL. Modeling action potential generation and propagation in NRK fibroblasts. *Am J Physiol C* 287, 851-865, 2004.
- Van Wijk van Brievingh** RP, Möller DPF (editors). *Biomedical Modeling and Simulation on a PC. A Workbench for Physiology and Biomedical Engineering*. Volume 6 of *Advances in Simulation*, Luker PA, Schmidt B (editors). Springer-Verlag, 1993.
- Weidema** AF, Ravesloot JH, Panyi G, Nijweide PJ, Ypey DL: A Ca²⁺-dependent K⁺-channel in freshly isolated and cultured chick osteoclasts. *Biochim Biophys Acta* 1149, 63-72, 1993.

Wiltink A, Nijweide PJ, Scheenen WJJM, Ypey DL, VanDuijn B. Cell membrane stretch in osteoclasts triggers a self-reinforcing Ca^{2+} entry pathway. *Pfluegers Arch - Eur J Physiol* 429, 663-671, 1995.

Ypey DL. Practical introduction to patch clamping by simulation experiments with simple electrical circuits. Chapter 7 in: *Signal Transduction - Single Cell Techniques*. B Van Duijn and A Wiltink (editors). Springer Verlag, Berlin-Heidelberg-New York, 52-87, 1998.